

**BEHAVIOR OF HYBRID FIBER REINFORCED
PRESTRESSED CONCRETE BEAMS UNDER
FLEXURE-SHEAR**

Suhas S Joshi

A Dissertation Submitted to
Indian Institute of Technology Hyderabad
In Partial Fulfilment of the Requirements for
The Degree of Master of Technology



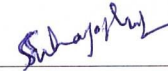
भारतीय प्रौद्योगिकी संस्थान हैदराबाद
Indian Institute of Technology Hyderabad

Department of Civil Engineering

Dec 2018

Declaration

I declare that this written submission represents my ideas in my own words, and where others' ideas or words have been included, I have adequately cited and referenced the sources. I also declare that I have adhered to all principles of academic honesty and integrity and have not misrepresented or fabricated or falsified any idea/data/fact/source in my submission. I understand that any violation of the above will be a cause for disciplinary action by the Institute and can also evoke penal action from the sources that have thus not been properly cited, or from whom proper permission has not been taken when needed.



(Signature)

Suhas S Joshi

CE16MTECH01001

Approval Sheet

This thesis entitled Behaviour of Hybrid fiber reinforced prestressed concrete beams under flexure-shear by Suhas S Joshi is approved for the degree of Master of Technology/ ~~Doctor of Philosophy~~ from IIT Hyderabad.



Dr. Gangadharan R

Department of Mechanical and Aerospace Engineering

Examiner



Dr. Anil Aggarwal

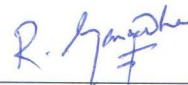
Department of Civil Engineering

Examiner



Dr. S. Suriya Prakash

Adviser



Dr. Gangadharan R

Chairman

Acknowledgments

I would like to express my sincere gratitude to my advisor Dr. S. Suriya Prakash, without his support and thoughtful guidance this research work would not have accomplished. He always tried to push my limits, due to which I have realized my potential to deliver the things.

I would like to express my sincere thanks to professors in the structural Engineering division, Prof. K V L Subramaniam, Dr. Anil Agarwal, Dr. A Rajagopal, Dr. Surendra Nadh Somala, Dr. Mahendra Kumar Madhavan, for enhancing my basic knowledge in structural Engineering and also providing exposure to practical aspects through term projects during course work. I would also like to thank Mr. Nikesh Thammishetti, Mr. Anand G Ganganagoudar, Mr. M. Chellapandian, Dr. Pradeep Kankeri, Mr. Saumitra Jain, Mr. Chandrashekhar Lakhavath, Mr. Aniket Bhosale, Mr. Sriharsha K and all other members of CASTCON (condition assessment and strengthening of concrete structures) research group for all the assistance provided during my research period. I would like to thank Mr. Gopal, Mr. Laxman, Mr. Prashanth, Mr. Venkatesh and Mr. Raju for their assistance in carrying out experimental work. Their assistance and effort to complete the experimental program is highly appreciated. I would also like to thank Government of India for providing financial assistance through the Utchattar Avikshkar Yojana (UAY) Scheme, PRECA India Pvt. Ltd for helping us with the casting process and Greenix Pvt.Ltd for sponsoring the fibers for this research work. Lastly, I would like to thank my family members for their continuous support and encouragement.

Thank you very much.

Dedicated to

My family and friends

Abstract

The present study aims at understanding the effect of hybridization of the steel and synthetic fibers on the flexure-shear behavior of prestressed concrete (PSC) beams. The first phase of the test program consists of evaluating the efficiency of individual fibers viz. steel and structural synthetic fibers on the performance of prestressed concrete (PSC) beams. Later, a hybrid fiber combination consisting of steel and synthetic fibers are introduced to understand the behavior. The effect of different fiber reinforcement on the behavior of prestressed concrete beams are evaluated in two stages. First, fracture tests are conducted to understand the influence of fibers at the material level. Secondly, full-scale prestressed concrete beams are tested for evaluating the effect of fiber addition on the flexure-shear behavior. The test matrix consists of seventeen beams with fiber reinforced concrete, having fiber dosages of 0.35%, 0.70% and 1.0% by volume of concrete. All the beam specimens are tested at a shear span (a) to depth ratio (d) of five under four-point bending configuration. Effect of hybrid fiber addition on the overall load-displacement, load-strain, and strain energy absorption capacity of PSC beams are analyzed. Other parameters such as shear span to depth ratio (a/d), the compressive strength of concrete, prestressing reinforcement ratio are kept constant. Results of hybrid fiber reinforced specimens is compared with the results of steel and Synthetic (polyolefin) fiber reinforced beams. The test results portray that the addition of fibers stiffen the post-cracking response and increases the energy absorption capacity. Additionally, failure mode changed from flexure-shear (brittle) to flexure (ductile) mode with the addition of fibers. Change of failure mode occurred at dosages of 0.35% for steel and hybrid fibers and 0.70% for synthetic (Polyolefin) fibers. The strain energy absorption capacity increased by more than 100% at 1.0% fiber addition for both steel and macro-synthetic fibers. Flexural capacity of the tested

specimens is verified with the RILEM recommendation for fiber reinforced concrete specimens. RILEM recommendations always underpredicted the actual value, indicating the conservative estimates of design guidelines. Cracking behavior of PSC beams are analyzed viz. crack width and crack spacing parameters using Eurocode, CEB-FIP modal code and Moffatt's modified formulation. It is observed that, as the fiber dosage is increased, corresponding crack widths are reduced in the post-cracking regime.

Notations

The following notations are used in this thesis:

The following symbols are used in the equations (1-15)

A_c = cross section of concrete (mm^2)

A_s = area of tension reinforcement is extending not less than “d + anchorage length” beyond the section considered (mm^2).

A_{sw} = area of shear reinforcement (mm^2).

b_f = the width of the flanges (mm)

b_y = minimum width of the section over the effective depth d (mm).

D = the depth of beam used in fracture test

D_{lig} = the depth of ligament in fracture test

d = effective depth (mm)

E_c = modulus of elasticity of concrete

f_{ck} = the characteristic compressive strength of cylinders in MPa

$f_{fcm,fl}$ = mean flexural tensile strength in MPa

$F_{R,j}$ = jth residual load

$f_{R,j}$ = jth residual strength

$f_{R,1}, f_{R,4}$ the residual flexural strength of FRC at CMOD of 0.5 mm and 3.5 mm, respectively

$f_{rk,4}$ = the residual flexural tensile strengths at CMOD = 3.5mm

f_{ywd} = the design yield strength of the shear reinforcement (N/mm^2).

h = overall depth (mm)

h_f = the height of the flanges (mm)

K_h = size factor

k_f = factor for taking into account the contribution of the flanges in a T-section

L = the span of the beam used in the fracture test

N_{sd} = longitudinal force in section due to loading or prestressing

s = the spacing between the shear reinforcement measured along the longitudinal axis (mm)

V_{cd} = the shear resistance of the member without shear reinforcement

V_{fd} = the contribution of the steel/synthetic fiber shear reinforcement

V_{Rd3} = the design shear resistance of a section of a beam

V_{wd} = the contribution of the shear reinforcement due to stirrups and inclined bars

α = the angle of the shear reinforcement with the longitudinal axis

τ_{fd} = design value of the increase in shear strength due to steel/synthetic fibers

Contents

| | |
|----------------------------------------------------------------------------------------------------|------------|
| Declaration..... | i |
| Approval Sheet..... | ii |
| Acknowledgments | iii |
| Abstract..... | v |
| Notations | vii |
| Chapter 1 Introduction..... | 1 |
| 1.1. General..... | 1 |
| 1.2. Why add fibers to the concrete? | 2 |
| 1.2.1. Different types of fibers | 3 |
| 1.2.2. Mechanical properties of fiber reinforced concrete | 5 |
| 1.3. Need for hybrid fiber addition | 7 |
| Chapter 2 Literature Review | 9 |
| Background..... | 9 |
| 2.1. Effect of shear span to depth ratio on the behavior of reinforced concrete (RC) members | 10 |
| 2.2. Behavior of fiber reinforced concrete under Different Loads | 11 |
| 2.2.1. Studies on steel fiber reinforced concrete | 11 |
| 2.2.2. Studies on synthetic fiber reinforced concrete..... | 12 |
| 2.2.3. Studies on hybrid fiber reinforced concrete..... | 13 |
| 2.3. The behavior of fiber reinforced prestressed concrete members | 14 |
| 2.4. Knowledge gaps from Literature Review | 21 |
| Chapter 3 Objectives and scope..... | 22 |
| 3.1. Background and research significance | 22 |
| 3.2. Objectives of the study | 23 |

| | |
|----------------------------------------------------------------------------------------|-----------|
| Chapter 4 Experimental program..... | 26 |
| 4.1. Material properties | 26 |
| 4.1.1. Fibers..... | 26 |
| 4.1.2. Concrete | 27 |
| 4.1.3. Internal reinforcement-prestressing steel strand | 29 |
| 4.2. Specimen preparation | 29 |
| 4.3. Test setup and Instrumentation | 30 |
| 4.3.1. Fracture tests on fiber reinforced concrete specimens | 30 |
| 4.3.2. Full-scale tests on fiber reinforced prestressed concrete beams | 31 |
| 4.3.3. Digital Image Correlation (DIC) technique | 33 |
| Chapter 5 Test results and Discussions..... | 35 |
| 5.1. General..... | 35 |
| 5.2. Fracture behavior of fiber reinforced concrete | 35 |
| Chapter 6 Analytical Study..... | 61 |
| 6.1. General..... | 61 |
| 6.2. Capacity calculation using RILEM recommendations | 61 |
| 6.2.1. Flexural moment capacity..... | 61 |
| 6.2.2. Shear capacity | 64 |
| 6.2.3. Capacity comparison..... | 66 |
| 6.3. Analysis of crack width and crack spacing in fiber reinforced concrete beams..... | 67 |
| 6.3.1. Introduction..... | 67 |
| 6.3.2. Crack spacing model based on RILEM TC162-TDF | 69 |
| 6.3.3. Crack spacing model based on CEB-FIP modal code | 71 |
| 6.3.4. Modified equations based on Moffat's crack spacing model..... | 72 |
| 6.3.5. Effect of modification factor in the formulae of RILEM and CEB-FIP code | 74 |

Chapter 7 Summary and Conclusion.....77

Reference

List of publications

List of Figures

| | |
|-------------------------------------------------------------------------------------------------------|----|
| Figure 1.1: Bricks are strengthened using straw | 1 |
| Figure 1.2: Steel fibers (Source: Dramix, Bekaert) | 3 |
| Figure 1.3: Glass fibers | 4 |
| Figure 1.4: Synthetic fibers..... | 4 |
| Figure 1.5: Natural fibers..... | 5 |
| Figure 1.6: Advantages of Fiber-reinforced concrete | 6 |
| Figure 2.1: Overview of the literature survey | 9 |
| Figure 2.2: Behavior of reinforced concrete beams at different shear span to depth (a/d) ratios | 10 |
| Figure 2.3: Load vs mid-span deflection response | 15 |
| Figure 2.4: Crack width (mm) variation for different shear reinforcement types | 16 |
| Figure 2.5: Cracking patterns..... | 16 |
| Figure 2.6: Specimens details | 18 |
| Figure 2.7: Flexure behavior of fully prestressed fiber reinforced concrete beams | 19 |
| Figure 2.8: Flexure behavior of partially prestressed fiber reinforced concrete beams | 19 |
| Figure 2.9: Crack width variation with applied load | 20 |
| Figure 3.1: Load vs. deflection curves from fracture tests | 23 |
| Figure 3.2: Brief overview of research work | 24 |
| Figure 3.3: Workflow of the research plan | 25 |
| Figure 4.1: Cylinder testing under compression..... | 29 |
| Figure 4.2: Casting process of fiber reinforced prestressed concrete beams..... | 30 |
| Figure 4.3: Fracture test setup..... | 31 |
| Figure 4.4: Schematic Details of the Test Specimen | 32 |
| Figure 4.5: Test setup and Instrumentations | 33 |

| | |
|--------------------------------------------------------------------------------------------------------------|----|
| Figure 4.6: Schematic plan view of DIC setup | 34 |
| Figure 5.1: Typical Load Vs. CMOD Curves of FRC | 37 |
| Figure 5.2: Behavior of control specimen (without fibers)..... | 38 |
| Figure 5.3: Flexure-shear failure of control specimens | 39 |
| Figure 5.4: Behavior of 0.35% dosage of steel fiber reinforced specimens | 40 |
| Figure 5.5: Flexure failure of SF35 specimen | 41 |
| Figure 5.6: Behavior of 0.7% dosage of steel fiber reinforced specimens | 41 |
| Figure 5.7: Flexure failure of SF70 specimen | 42 |
| Figure 5.8: Behavior of 1.0% dosage of steel fiber reinforced specimens | 43 |
| Figure 5.9: Flexure failure of SF100 specimen | 43 |
| Figure 5.10: Deflection measurements from DIC analysis and compared with LVDT readings | 45 |
| Figure 5.11: Longitudinal strain contours (DIC) on the horizontal line a-b before and after cracking..... | 47 |
| Figure 5.12: Average Strain along the level of the crack tip at failure | 47 |
| Figure 5.13: Behavior of 0.35% dosage of polyolefin fiber reinforced specimens | 48 |
| Figure 5.14: Flexure-shear failure of PO35 specimen | 48 |
| Figure 5.15: Behavior of 0.70% dosage of polyolefin fiber reinforced specimens | 49 |
| Figure 5.16: Flexure behavior of PO70 specimen | 50 |
| Figure 5.17: Behavior of 1.0% dosage of polyolefin fiber reinforced specimens | 51 |
| Figure 5.18: Flexure behavior of PO100 specimen | 51 |
| Figure 5.19: Behavior of 0.35% dosage of hybrid(SF+PO) fiber reinforced specimens..... | 52 |
| Figure 5.20: Flexure behavior of HB35 specimen..... | 53 |
| Figure 5.21: Behavior of 0.70% dosage of hybrid(SF+PO) fiber reinforced specimens..... | 53 |
| Figure 5.22: Flexure behavior of HB70 specimen..... | 54 |
| Figure 5.23: Behavior of 1.0% dosage of hybrid(SF+PO) fiber reinforced specimens..... | 54 |

| | |
|-------------------------------------------------------------------------------------------|----|
| Figure 5.24: Flexure behavior of HB100 specimen..... | 55 |
| Figure 5.25: Load-deflection behavior of fiber reinforced prestressed concrete beams..... | 56 |
| Figure 5.26: Failure modes of PSC beam with different fibers/dosages | 57 |
| Figure 5.27: Load-strain (strand) behavior of PSC beams | 59 |
| Figure 5.28: Normalized energy absorption capacity of the specimens | 60 |
| Figure 6.1: Flexural capacity calculation..... | 63 |
| Figure 6.2: Shear resistance of FRC | 64 |
| Figure 6.3: Fiber reinforced prestressed concrete beam details..... | 68 |
| Figure 6.4: Result from sectional analysis using RILEM recommendations | 69 |
| Figure 6.5: Crack width calculation using RILEM(Euro code) recommendation..... | 71 |
| Figure 6.6: Crack width calculation using CEB-FIP (1993)..... | 72 |
| Figure 6.7: Moffatt's model..... | 74 |
| Figure 6.8: Influence of Moffatt's modification factor..... | 76 |

List of Tables

| | |
|-----------------------------------------------------------------|----|
| Table 4.1: Properties of Steel and macro-synthetic fibers | 27 |
| Table 4.2: Mix design details | 28 |
| Table 4.3: Details of concrete specimens | 28 |
| Table 5.1: Residual flexural strength of FRC specimens | 37 |
| Table 6.1: Capacity comparison | 67 |

Chapter 1

Introduction

1.1. General

Fiber reinforced concrete (FRC) is tailored by the addition of randomly oriented fibers to plain concrete. Addition of fibers to enhance the properties of building materials is relatively not new and has been practiced since ancient times. Straw and horse-hair were used to reinforce mud bricks and mortar, respectively (Figure 1.1). With the evolution of the new manufacturing technologies, researchers have developed novel reinforcing materials such as steel fibers (plane and hooked end), synthetic fibers, and natural fibers. The composite resulting from the addition of fibers to concrete exhibits improved mechanical properties compared to that of plain concrete.



Figure 1.1: Bricks are strengthened using straw

(Source: <https://fugahumana.files.wordpress.com/2012/07/mud-and-straw-brick.jpg>)

ACI Building Code 318 [1] permits the design engineers to use steel fiber reinforced concrete (SFRC) as a replacement to conventional shear reinforcement. However, ACI code

mandates that SFRC beams are required to have a minimum steel fiber dosage of 0.75% in volume and compressive strength not greater than 42 MPa. This mandate is because current ACI provisions are primarily based on experimental studies on non-prestressed concrete beams cast of concrete with cylinder compressive strength less than 42 MPa. However, in a prestressed concrete beam, the beneficial effect of prestressing forces could further relax the minimum required fiber volume fraction and can make the use of SFRC more economical. Thus, the focus of this investigation is to study the effect of steel fibers on the cracking and ductility behavior of prestressed concrete beams under flexure/flexure-shear.

1.2. Why add fibers to the concrete?

Usage of fiber reinforced concrete (FRC) has been continuously increasing in the construction industry due to its various advantages such as improvement in post-cracking stiffness, flexural toughness and ease of availability at a competitive price. Moreover, the usage of prestressed concrete in the construction requires high strength concrete, which is highly catastrophic. Hence the usage of fibers in high strength concrete can mitigate the brittle nature by enhancing the ductility properties. Different fibrous materials have different mechanical properties, and hence the selection of fiber depends on the property of the concrete which is to be enhanced. Steel FRC is mainly used in the seismic resistant structures, tunnel construction, blast, and impact resistant structures where the post-cracking behavior is of major concern. Apart from crack resistance, steel fibers can also be used to replace the conventional transverse reinforcement in the concrete. Nowadays light weight fibers such as synthetic fibers (ex: polyolefin, polypropylene fibers) are also used to control the crack, increase the ductility and thereby improve the overall performance of the concrete.

1.2.1. Different types of fibers

Steel fibers: Steel fibers are widely used in the construction practice due to several advantages, such as high tensile strength (345-3000 MPa), high elastic stiffness (200 GPa). Steel fibers (Figure 1.2) reduces the crack width of the concrete by bridging the cracked faces in the serviceability regime. Aspect ratio and diameter of the steel fibers vary in between 30 to 250 and 0.25mm to 0.75 mm respectively. Steel fibers are ductile; they can undergo elongation up to 4-10%.



Figure 1.2: Steel fibers (Source: Dramix, Bekaert)

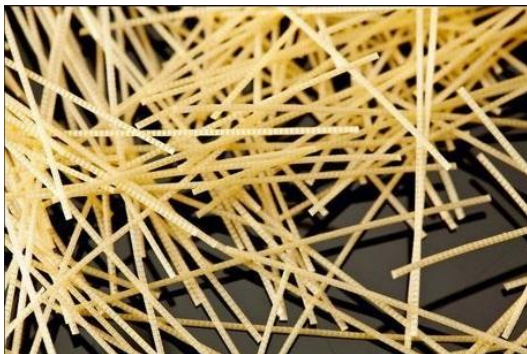
Glass fibers: Glass fibers are light weight compared to the steel fibers, as the specific gravity of glass fibers are 2.5. The tensile strength of fibers varies between 1000-2600 MPa, and Young's modulus is in the range of 70-80 GPa. Presence of glass fibers in the concrete improves the flexural strength and provide resistance to thermal shock. Glass fibers are brittle. Hence, it will undergo the ultimate elongation up to 1.5-3.5% only.



Figure 1.3: Glass fibers

(Source : <https://www.expressions-ltd.com/products/gfrc-ar-glass-fiber-chopped>)

Synthetic fibers: These are the fibers produced from the textile and petrochemical industry. Synthetic fibers are generally used in cladding panel and shotcrete application. These fibers are very light weight; specific gravity is in the range of 0.9-0.96, which is less than that of water. Synthetic fibers (Figure 1.4) have a low modulus of elasticity (10 GPa). Micro synthetic fibers (Figure 1.4b), when used in concrete, reduces the shrinkage and thermal cracks, whereas macro synthetic (Figure 1.4a) variants help to improve the ductility of the concrete members.



a) Polyolefin fiber



b) Polypropylene fiber

Figure 1.4: Synthetic fibers (source: <https://www.contecfiber.com/en/products/concrix>)

Natural fibers: Natural fibers have high impact strength and these fibers are produced at lower cost. These fibers may undergo organic decay. Sisal, coconut and jute fiber are the few

examples (Figure 1.5) of natural fibers. Specific gravity varies between 0.68-1.1, and tensile strength is in between 100-800 MPa.



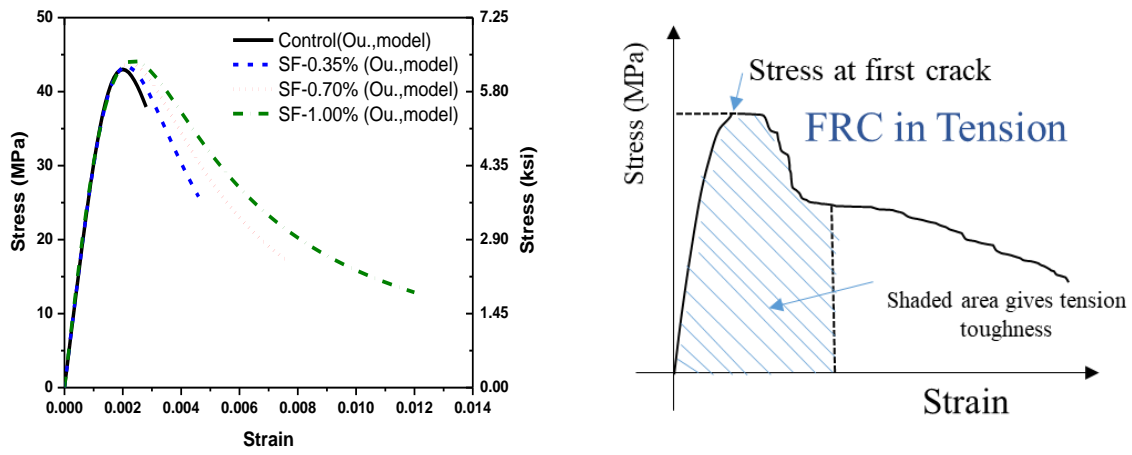
Figure 1.5: Natural fibers (source: <https://carriagehousepaper.com/sisal-fiber>)

1.2.2. Mechanical properties of fiber reinforced concrete

Figure 1.6a shows the results of concrete cylinder stress-strain curves with and without fibers under compression. The addition of steel fibers was found to significantly improve the strength and stiffness degradation in the post-peak region with better ductility (Figure 1.6a). Previous works [2]–[5] have also confirmed the same at both the room and moderate temperature exposure. The behavior of concrete in tension: The failure pattern in the control specimen is predominantly due to a single explicit crack at the center of the specimen. This observation indicates that the stress concentration in the crack region reduces the post-cracking load resistance of the specimen. On the other hand, the FRC specimen shows a similar large crack at failure, but the crack opening was delayed due to the presence of fibers in the section (Figure 1.6b).

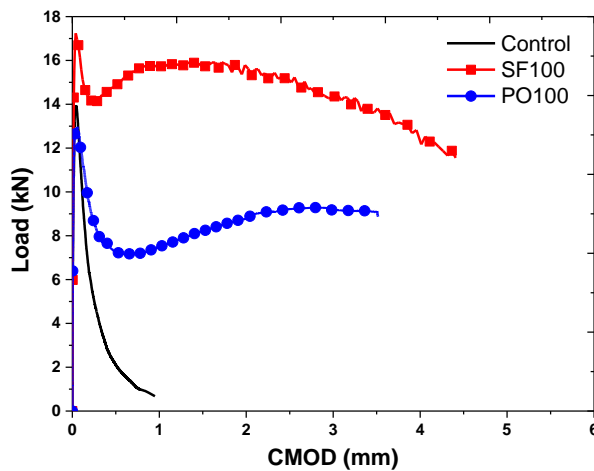
Fracture behavior: Understanding the fracture behavior of fiber reinforced concrete (FRC) is essential for its inclusion in structural design. Fracture tests were conducted to evaluate the

efficiency of different fibers. Crack mouth opening displacement is one of the parameters to evaluate the fracture behavior of concrete. The load vs. CMOD curves (Figure 1.6c) indicate that fibers restrict the crack opening more efficiently than that of the specimen without fibers. The difference in the performance of different fibers is due to the mechanical and geometrical properties of the fibers. The load drop after the peak load is minimum in case of steel fiber reinforced specimen due to higher elastic modulus and tensile strength of steel fiber.



a) FRC in compression [2]

b) FRC in tension



c) Fracture behavior of FRC [3]

Figure 1.6: Advantages of Fiber-reinforced concrete

1.3. Need for hybrid fiber addition

Though steel fibers have superior mechanical properties compared to that of synthetic fibers, they decrease the workability and creates the balling effect at a higher dosage. On the other hand, structural synthetic fibers, being non-corrosive and malleable, have gained attention in recent years. Each of the available fibers has its advantages as well as disadvantages. The efficient usage of different fibers can be obtained through fiber hybridization [6].

Hybrid fiber system can be of different types, such as

- (a) Combination of fibers with different stiffness properties
- (b) Combination of fibers with different lengths
- (c) Combination of fibers with different durability properties

(a) Combination of fibers with different stiffness properties: The hybrid combination, with fibers of different stiffness properties, is found to enhance the load carrying and strain energy absorption capacities. Also, the addition of synthetic fibers with steel helps in countering the significant reduction of the workability in the fresh state without compromising the structural performance at hardened state. The fibers with higher stiffness are found to enhance the cracking load and ultimate capacity whereas the fibers with lower stiffness improve the toughness and strain absorption capacity in the post-cracking regime.

(b) Combination of fibers with different lengths: The fibers of smaller lengths control the formation and growth of microcracks which in turn improves the tensile strength of the

concrete. The fibers of larger lengths bridge the macrocracks and improve the overall ductility of the concrete.

(c) Combination of fibers with different durability properties: Highly durable fibers provide the strength and toughness retention for long-term and the fibers with less durability control the short-term performance (transportation + installation) of the concrete composite.

Organization of the thesis:

The 2nd chapter presents an overview of the literature survey related to this research. It describes the previous works on the behavior of fiber reinforced prestressed concrete. Also, the fracture behavior of steel, synthetic, and hybrid fiber reinforced concrete. Chapter 3 presents the objectives and scope of the present experimental studies. Chapter 4 discusses the material properties, test setup, and instrumentation details. Chapter 5 describes the results of experiments and assesses the behavior of fiber reinforced prestressed concrete, which are reinforced with steel, synthetic and hybrid fibers. It provides the complete details of load-deflection curves, load-strain curves, and failure modes. The efficiency of different fibers was evaluated using fracture tests. The effect of hybridization of steel and synthetic fibers on the flexure-shear behavior is also presented. Chapter 6 presents the capacity calculations of fiber reinforced concrete specimens using RILEM recommendations. Additionally, cracking behavior such as crack width and crack spacing is also studied. Finally, Chapter 7 presents the summary and conclusions from the experimental investigation.

Chapter 2

Literature Review

Background

Flexure, shear and combined flexure-shear behavior of concrete members internally reinforced with discrete fibers have been extensively studied from literature and are presented in this section. Based on the literature review, the objectives arrive for the present study were studied with the scope of experimental and analytical work. The sequence followed in the literature survey is shown in Figure 2.1.

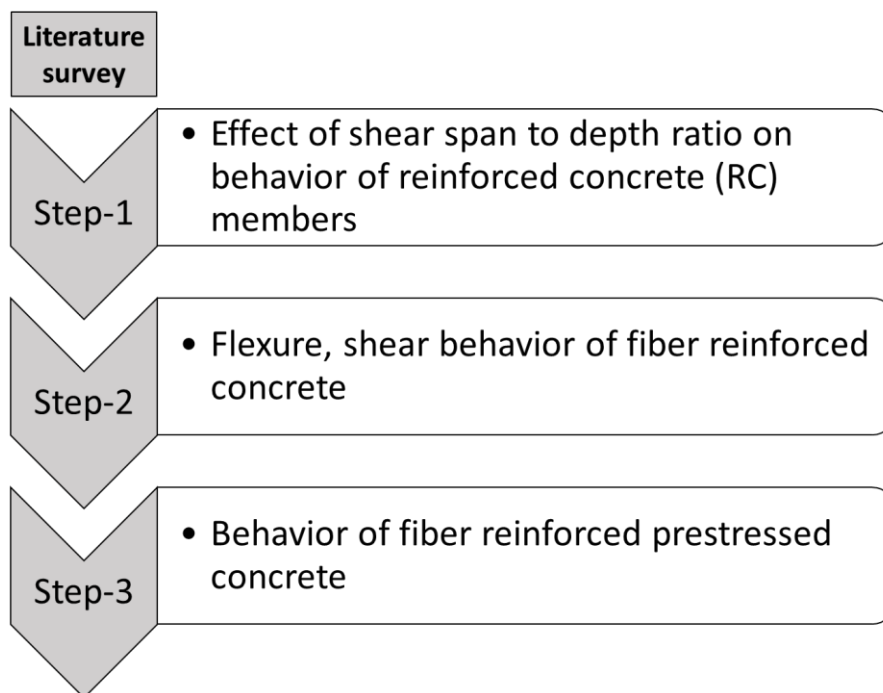
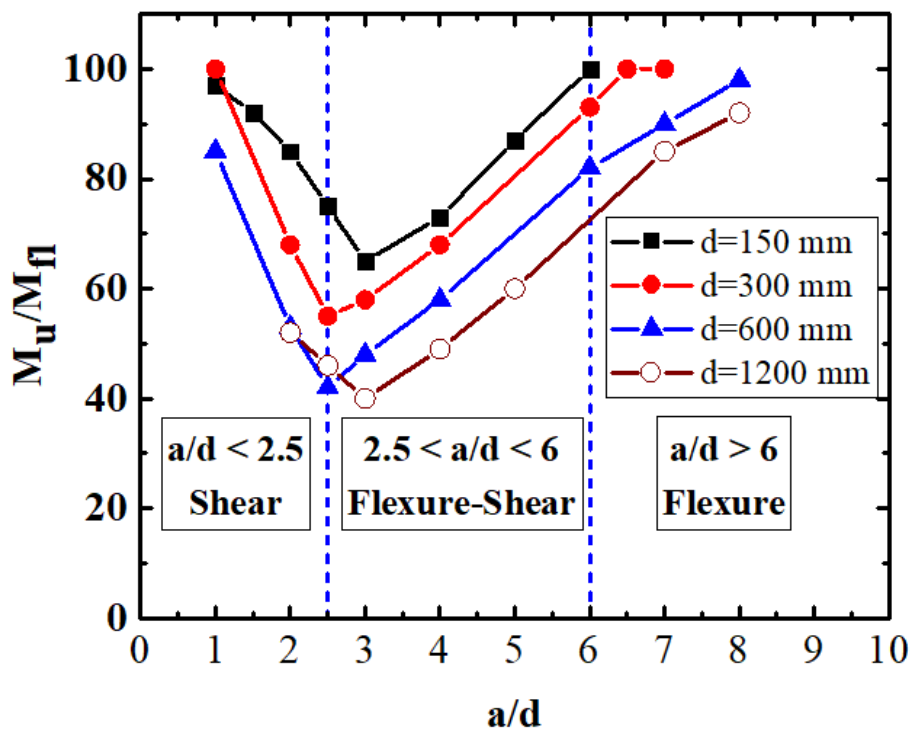


Figure 2.1: Overview of the literature survey

2.1. Effect of shear span to depth ratio on the behavior of reinforced concrete (RC) members

Kani [7] investigated the effect of different a/d ratios on the behavior of reinforced concrete (RC) beams (Figure 2.2). The author found that the beams had dominant flexure behavior above a/d ratio of 6. The author also observed that the a/d ratio of 2.5 is a transition point below which the beams are shear critical and the corresponding bending moment at failure was found to be minimum. Below the a/d ratio of 2.5, the beam is shown to develop an arch action with a considerable reserve strength beyond the first cracking point. Additionally, for a/d ratio between 2.5 and 6, the failure was due to sudden diagonal shear tension and flexure-shear mode.



Note: a = shear span, d = effective depth

Figure 2.2: Behavior of reinforced concrete beams at different shear span to depth (a/d) ratios

2.2. Behavior of fiber reinforced concrete under Different Loads

2.2.1. Studies on steel fiber reinforced concrete

Ding et al. [8] studied the composite effect of steel fibers and stirrups on the shear behavior of beams using self-consolidating concrete (SSC). For this, he conducted tests on a series of simply supported SCC rectangular beams using steel fiber reinforcement with and without stirrups with varying fiber content and stirrup ratios.

The few interesting observations from the experiments are

- As the fiber content is increased, there is a significant increase in shear strength and the addition of steel fibers in an adequate percentage changed failure mode from brittle shear collapse to a ductile flexural mechanism.
- Combination of stirrups and steel fibers provided a positive hybrid effect on the mechanical behavior which can be used to enhance the flexural and shear resistance and to replace the stirrups of RC members

Yoo et al. [9] studied the effects of the stirrup, steel fiber and beam size on shear behavior of high strength concrete beams. To investigate shear behavior, the authors tested six large scale reinforced high strength concrete (HSC) beams with and without stirrups with a/d ratio of 3.2, 0.75% volume of steel fibers.

From test results, the authors noted that

- When beam size increased, a significantly lower shear strength was observed for fiber reinforced HSC beams without stirrups than for plain HSC beams with stirrups.
- Additionally, they have also noted that use of steel fibers effectively limited crack propagation, produced more diffused initial flexural cracks, leading to higher post-cracking stiffness, compared to plain HSC. However, the use of minimum stirrups gave

better shear cracking behaviors than that of steel fibers and effectively mitigated the size effect on shear strength.

Singh [10] presented the flexural modeling of steel fiber reinforced concrete (SFRC) to determine the ultimate capacity, crack width of rectangular sections using strain compatibility and force equilibrium equations. Additionally, a normalized design chart for strength calculations considering the random distribution of fibers and other fiber parameters was also presented. Sahoo et al. [11] evaluated the effect of steel fibers on the behavior of concrete beams with and without stirrups. They noted a minimal increase in flexural capacity when the fiber dosage was more than 0.5%.

Fantilli et al. [12] observed an increase in tensile and compressive ductility due to the addition of fibers to concrete. They attributed the increase in ductility in compression to the passive confinement provided by the steel fibers. Harajli [13] studied the bond behavior of steel fiber reinforced concrete under static and cyclic loading. The author noted that the addition of steel fibers improved the bond strength, reduced the damage and increased the energy dissipation capacity under cyclic loading. Abbas and Khan [14] conducted fiber pull-out tests to study fiber-matrix interfacial behavior of hooked end steel fiber-reinforced concrete. They concluded that the ultimate pull-out load was found to increase with an increase in fiber size and embedment length.

2.2.2. Studies on synthetic fiber reinforced concrete

Alhozaimy et al. [15] investigated the mechanical properties and effects of pozzolanic materials on concrete reinforced with fibrillated polypropylene fibers of low volume fractions (< 0.3%).

They reported that fiber content variation had no significant effect on the compressive and flexural strength of FRC but improved its toughness and impact resistance. Yazdanbakhsh et al. [16] carried out analytical studies to predict the shear capacity of synthetic fiber reinforced concrete beams based on the model originally developed for steel fiber reinforcement. They noted that shear capacities from RILEM 162-TDF [17] recommendations were found to be more conservative than Fib-MC2010 [18] for synthetic fiber reinforced beams. Amin et al. [19] reported the material characterization of macro synthetic fiber reinforced concrete through a series of tension tests such as uniaxial tension test, round panel test. The authors concluded that the degree of variability in the results is lowest in the case of round panel tests compared to uniaxial tension tests.

2.2.3. Studies on hybrid fiber reinforced concrete

Yao et al. [20] evaluated the performance of three different hybrid fiber combinations at the same volume fraction (0.5%). They investigated the hybrid combinations of (i) steel fibers (SF) and polypropylene fibers (PP), (ii) steel fibers and carbon fibers (CF), and (iii) PP and CF. Moreover, significant improvement in the performance using a hybrid combination was reported when compared to the individual fiber addition. Among the three hybrid combinations, the CF, SF combination gave the best performance, due to similar elastic modulus and better synergy.

Studies by Lee et al. [21] have shown that the hybrid fiber reinforced concrete, reinforced with 0.4% dosage of nano-synthetic fiber and 20 kg/m³ of steel fibers met the residual tensile strength requirement specified by RILEM standards for the complete replacement of steel rebars. Later, Sahoo et al. [22] studied the influence of steel and polypropylene fibers on the

flexural behavior of reinforced concrete beams. The test results portrayed an improvement of 25-100% in flexural tensile strength due to the addition of steel or steel and synthetic (SF+PP) combination when compared to plain concrete.

2.3. The behavior of fiber reinforced prestressed concrete members

Tiberti et al. [23] studied the influence of concrete strength on the crack development of steel fiber reinforced concrete (SFRC) members and found that the usage of fibers led to reduced mean crack spacing in high strength concrete (HSC) when compared to normal strength concrete (NSC). They also noted that the influence of HSC and the presence of fibers requires further research to establish a stabilized crack pattern.

Cuenca et al. [24], [25] used steel fibers to control the crack propagation in precast beams and hollow core slabs. In the case of beams tested at a shear span to depth ratio (a/d) of three, they observed that the fibers and stirrups had a synergic effect resulting in better crack control mechanisms and enhanced tension stiffening. Whereas in the hollow core slabs with fibers an increase in the ultimate loads, as well as improved ductility, was observed when compared with the control specimens.

Key findings:

Load vs. midspan deflection graph indicates that

- The specimens with only fibers (HF600/5, HF400/7, and HF260/9) and only stirrups (H600TR/3) exhibited brittle failure. The difference in the post-peak behavior between the two series of beams is minimal (Figure 2.3).
- The beams exhibited improved ductility regarding post-peak behavior when the beams were reinforced with both stirrups and fibers (HF600TR/1).

Crack width variation (Figure 2.4) for different shear reinforcement types:

- Specimen with only stirrups were observed (Figure 2.5) to have very few cracks with a wider crack width than specimens with only fibers where fibers initiated distributed cracks.
- The average crack angle observed in all the series of beams was found to be in the vicinity of 22° .
- There was an improvement in the maximum load by 35% for the same crack width when both stirrups and fibers are introduced in the prestressed concrete beam.

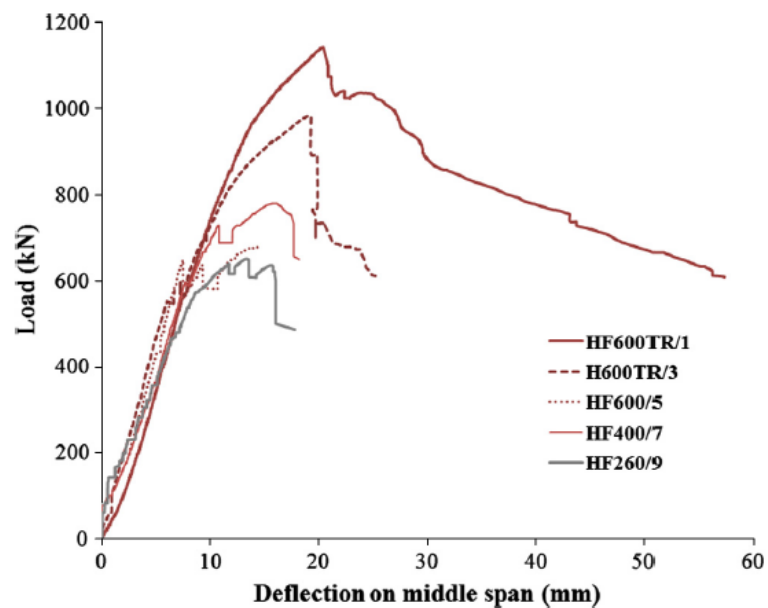


Figure 2.3: Load vs mid-span deflection response (Source: Cuenca et al. [24])

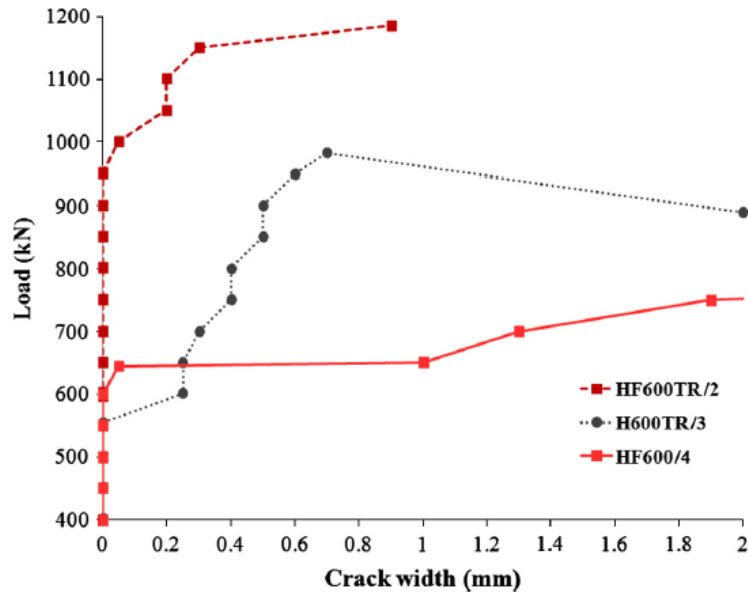


Figure 2.4: Crack width (mm) variation for different shear reinforcement types (Source: Cuenca et al. [24])

| <i>BEAM</i> | | | |
|-------------|---------------------------------------------|----------|---------|
| | HF600TR/2 | H600TR/3 | HF600/4 |
| | | | |
| | Load level for each crack line color | | |
| | 750 kN | 600 kN | 600 kN |
| | 900 kN | 700 kN | 700 kN |
| | 1100 kN | 800 kN | 750 kN |
| | FAILURE | | |

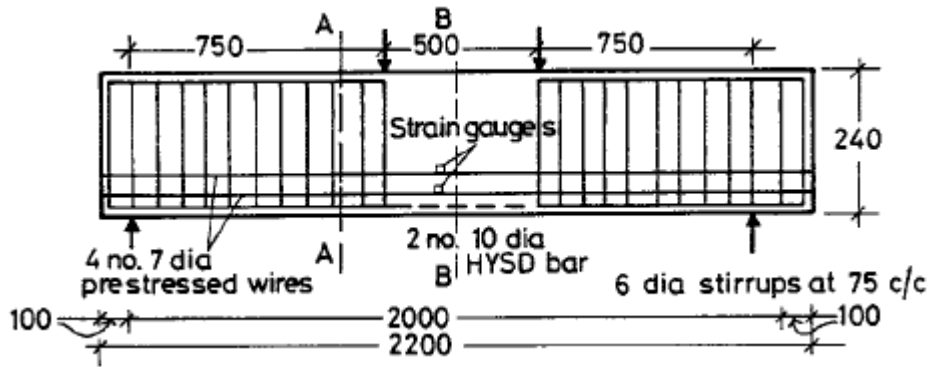
Figure 2.5: Cracking patterns (Source: Cuenca et al. [24])

Additionally, the authors calculated the shear capacity using different codal provisions for fiber reinforced concrete specimens. It is interesting to note that the code does not consider the influence of the fibers on the crack inclination (θ). Hence the fiber contribution is separately considered in the capacity calculation. The results from RILEM [17] and MC2010 [18] approach were found to be a function of the longitudinal reinforcement ratio. Moreover, all code provisions underestimate the fiber contribution to shear resistance.

Padmarajah and Ramaswamy [26] studied the effect of trough-shaped steel fibers on the flexural behavior regarding cracking and ultimate flexural capacity, load-deflection, moment-curvature, ductility, and energy absorption capacity of the full/partially fiber reinforced prestressed concrete specimens (Figure 2.6). The authors considered the amount of prestressing force, volume fraction (0%, 0.5%, 1.0%, and 1.5%) and location of the fibers over the depth of the beam as the main parameters in the test program. Analytical models to predict load-deflection and moment-curvature as a function of volume fraction were proposed.

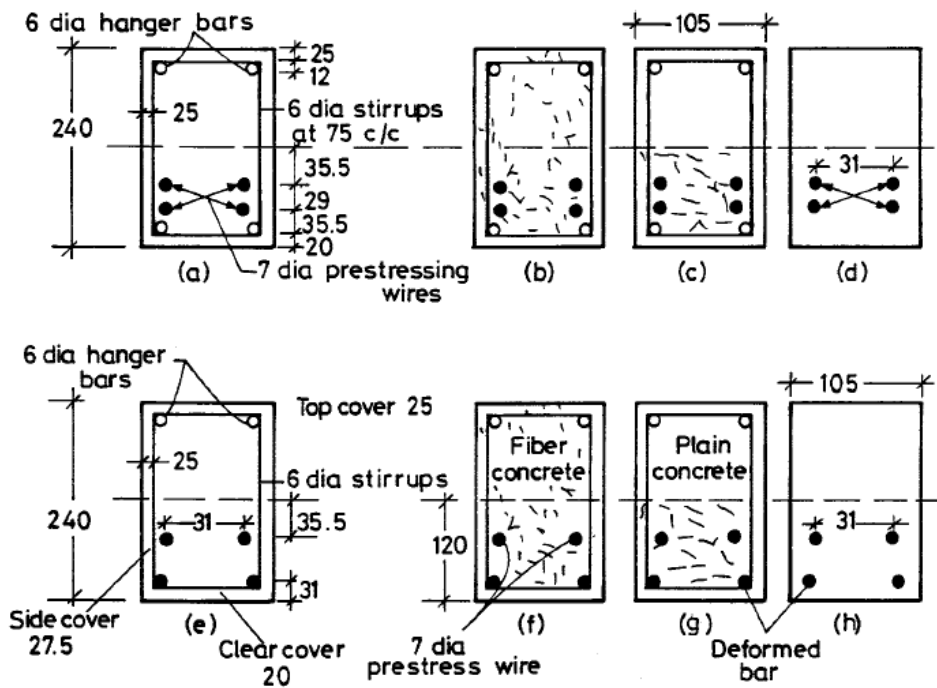
Main findings

- Members with the partial depth of steel fibers in the tension zone provided equal flexural capacity as that of the beam with the same dosage of fibers over the full depth. However full depth fiber reinforced beams were found to have enhanced ductility characteristics and improved structural integrity of the members.
- With the increase in fiber dosage, cracking load, ultimate load capacity and post-cracking stiffness improved.
- Partially prestressed members failed due to yielding of deformed steel rebars and concrete spalling in compression.
- The curvature of the fiber reinforced members was noticeably reduced due to fiber inclusion.
- The analytical model proposed in this work predict the behavior regarding load-deflection, moment-curvature reasonably.
- The ductility ratio defined as the ratio of deflection corresponding to the 80%-90% of peak load(after peak) to the deflection at cracking, is found to be higher in the case of full depth fiber reinforced beams compared to the partial depth FRC beam specimens.



(all dimensions are in mm)

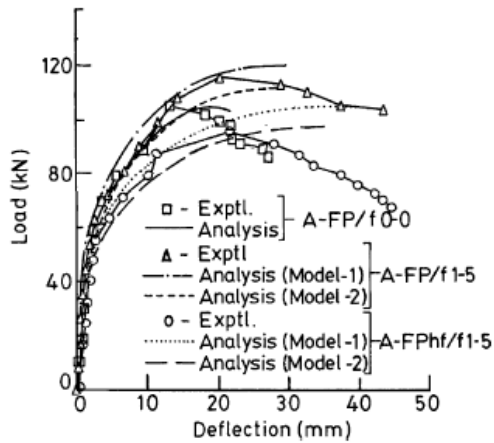
a) Test setup



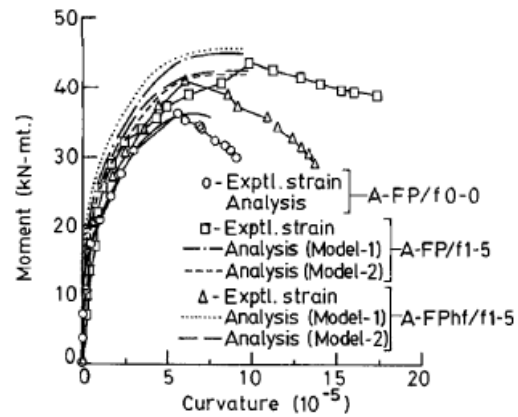
(all dimensions are in mm)

b) cross-sectional details of the specimen

Figure 2.6: Specimens details (source : Padmarajaih and Ramaswamy [27])

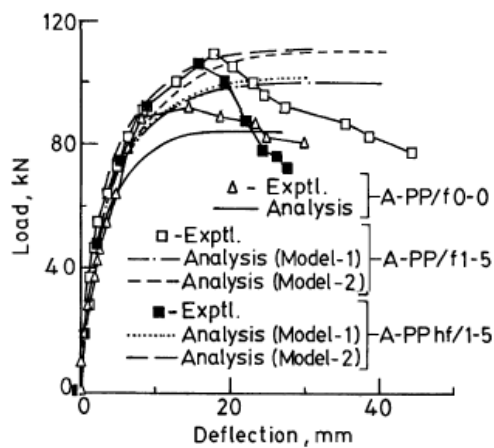


a) Load-deflection response

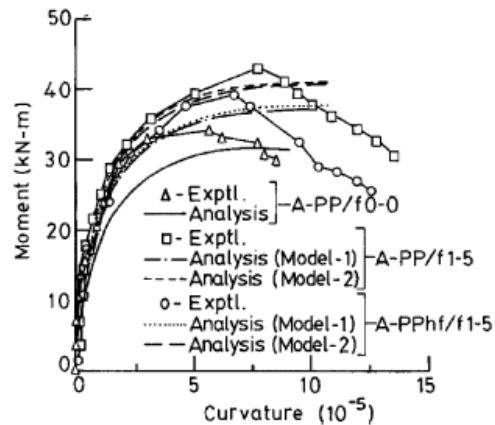


b) Moment-curvature response

Figure 2.7: Flexure behavior of fully prestressed fiber reinforced concrete beams (source: Padmarajaih and Ramaswamy [27])



a) Load-deflection response



b) Moment-curvature response

Figure 2.8: Flexure behavior of partially prestressed fiber reinforced concrete beams (source: Padmarajaih and Ramaswamy [27])

Furthermore, the same authors [27] proposed an analytical model to predict the crack width in partially and fully prestressed concrete beams with different dosage of steel fibers (Figure 2.9). They found that the addition of fibers restricted the crack initiation and propagation, eventually leading to an increase in the ultimate flexural strength.

Some of the inferences from this study are as follows:

- The proposed model predicted the experimentally measured crack width values very well up to 80% of the peak load.
- Presence of fibers reduced the steel strain at a given load as a function of fiber dosage.
- There was an enormous increase in stress redistribution in the case of fiber reinforced beam as compared to the beam having plain concrete only, due to which the crack width is reduced, and the number cracks were increased.
- The beneficial effect of prestressing force delayed the crack initiation in the case of fully prestressed concrete beam compared to the partially prestressed ones.
- All the fiber reinforced prestressed concrete beams failed with a flexure dominant crack in the pure bending zone and pull out of fibers were observed across the failure surface.
- The crack width value ranges for fully prestressed case varies between 0.8mm to 1.01mm for 0.5% dosage, 1.20 mm to 1.91 mm for 1.0% and 1.5% dosage. For the case of the partially prestressed beam, the crack width values were between 0.9mm to 2.4mm.

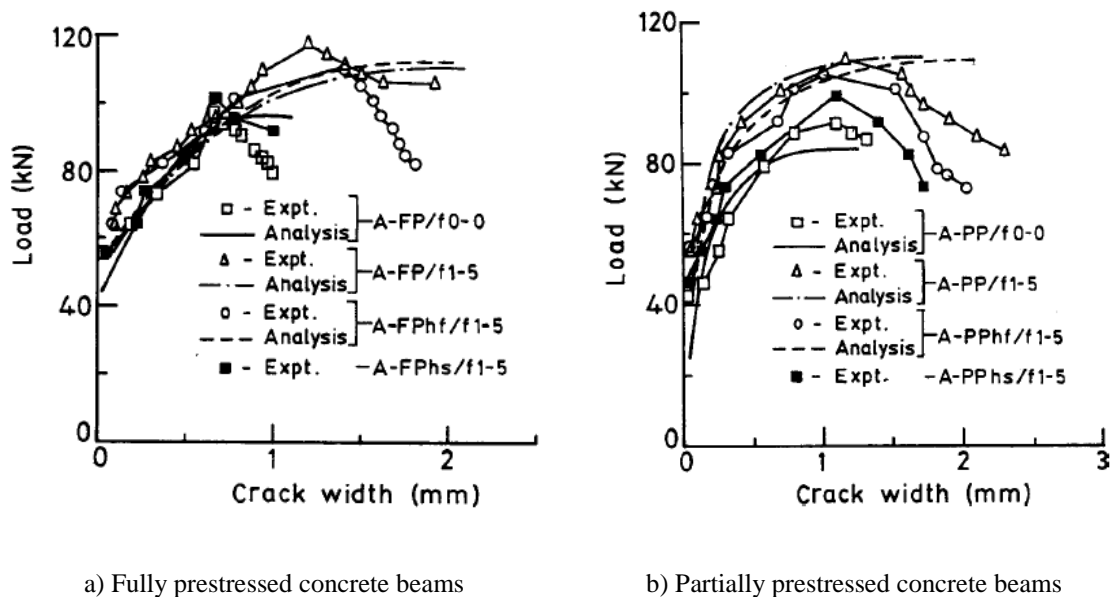


Figure 2.9: Crack width variation with applied load (source: Padmarajaih and Ramaswamy [27])

Antonio Conforti [28] studied shear behavior of prestressed double-tee section containing self-compacting polypropylene fiber reinforced concrete. To investigate shear behavior, six prestressed double tees in SCC and self-compacting polypropylene fiber reinforced concrete were tested. Shear tests were conducted in areas where the prestressing is uniformly distributed and at the end zones (which are more critical in shear as the beneficial effects of prestressing are not active) and observed web-shear cracking failure in the zone with uniform prestressing, flexural-shear cracking failure with a secondary splitting crack at the end zones. The authors concluded that macro-synthetic fibers could be used as shear reinforcement both in the zone with uniform prestressing (minimum shear reinforcement) and in the end zones (shear reinforcement required by equilibrium).

2.4. Knowledge gaps from the Literature Review

Most of the studies available in literature focused on the behavior of concrete elements reinforced with steel fibers and fibrillated or micro-synthetic fibers. Very limited studies are available on the performance of structural synthetic (polyolefin) fibers and a hybrid combination of steel and synthetic fibers on the flexure, shear and flexure-shear behavior of prestressed concrete beams. Thus, the proposed work tries to fill in in this knowledge gap by experimental work on prestressed concrete beams reinforced with different fibers. In the subsequent chapter, the significance and objectives of the present research program on the flexure-shear behavior of hybrid fiber reinforced prestressed concrete beams has been presented.

Chapter 3

Objectives and scope

3.1. Background and research significance

Fracture behavior is a multi-scale process, where each type of fiber can facilitate crack arresting at one strain level or within a limited range of strain. Therefore, to enhance the overall performance of FRC and to increase the effectiveness of fibers, the optimization of fiber dosage is essential for various fiber types and combinations. Steel FRC has been found to show better performance within small crack mouth opening displacement (CMOD) values with a quick load recovery after the cracking. However, the load drop is significant for the synthetic (Polyolefin) fiber reinforced concrete (SynFRC) after first cracking. Load resistance in SynFRC occurred at the higher values of CMOD. The difference in the performance of these fibers is due to the difference in elastic stiffness of fibers, adhesion with concrete and other geometrical properties of the fibers. Therefore, understanding the fracture behavior of hybrid fiber reinforced concrete (HFRC) is essential for its inclusion in structural design. Fracture tests conducted by Aniket et al. (2018) [3], indicated that steel fibers restrict the crack opening better than polyolefin fibers. Usage of hybrid fiber combination tends to shift the curve towards that of the steel fiber reinforced specimen (Figure 3.1), indicating better synergy between steel and synthetic fibers.

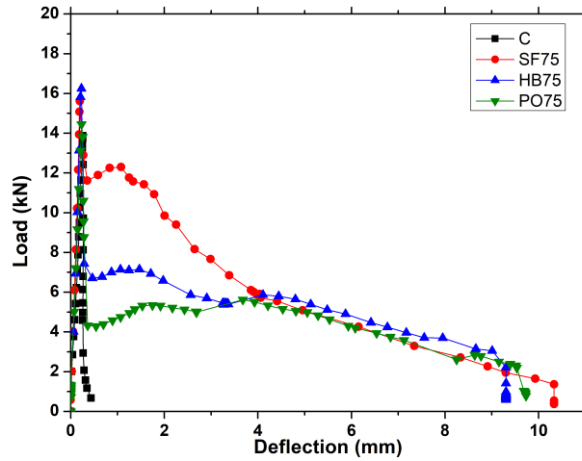


Figure 3.1: Load vs. deflection curves from fracture tests (Source: Aniket et al. [3])

Various factors like shear span to depth (a/d) ratio, compressive and tensile strengths of concrete and fiber dosage influence the performance of fiber reinforced concrete elements. Even though Kani's [7] studies are limited to reinforced concrete beams, only limited works in the past have focused on the effect of different a/d ratio on the behavior of prestressed concrete beams. Present work is a part of the large research program on the effect of different a/d ratio and fiber influence on the behavior of prestressed concrete beams. In the present case, a higher a/d ratio of five is considered to study the influence of steel and synthetic fibers on the flexure-shear behavior.

3.2. Objectives of the study

Steel fibers contribute to improved post-cracking behavior through increased ductility, multiple crack formation/crack distribution, reduced crack width and enhanced toughness properties. The review of the literature has revealed that most of the previous works mainly focused on the flexure/shear behavior of steel and fibrillated micro-synthetic fiber reinforced concrete. Inadequate information is available on the effect of structural synthetic fibers (polyolefin) and hybrid fiber (steel+ macro synthetic fiber) on the flexure, shear and flexure-shear behavior of prestressed concrete beams and is the focus of this investigation.

In the present study, the effect of different fiber reinforcement and its dosage on the behavior of prestressed concrete beams is investigated in two stages. Firstly, through Fracture tests, to understand the influence of steel, polyolefin and hybrid fiber addition to concrete at the material level. In the second phase, full-scale fiber reinforced prestressed concrete beams were tested to evaluate the flexure-shear response. Different fiber dosages such as 0.35%, 0.70% and 1.0% by volume of concrete were used. Furthermore, the effect of hybrid fiber inclusion is compared with that of individual fiber reinforced specimens of the same fiber dosages. Crack distribution, post-cracking stiffness and strain variation in the prestressing strand, energy absorption capacity and deflection were also compared to evaluate the efficiency of hybrid fibers concerning steel and synthetic fibers. A brief overview of the research work and workflow research plan is represented in Figure 3.2 and Figure 3.3 respectively.

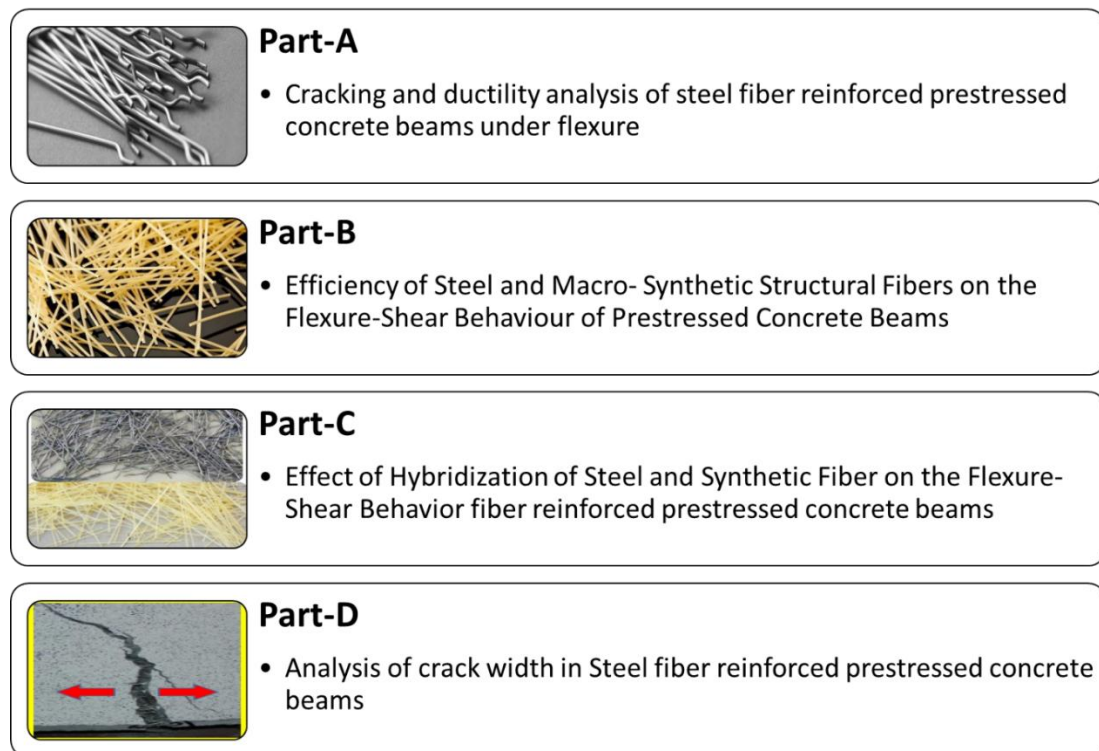


Figure 3.2: Brief overview of research work

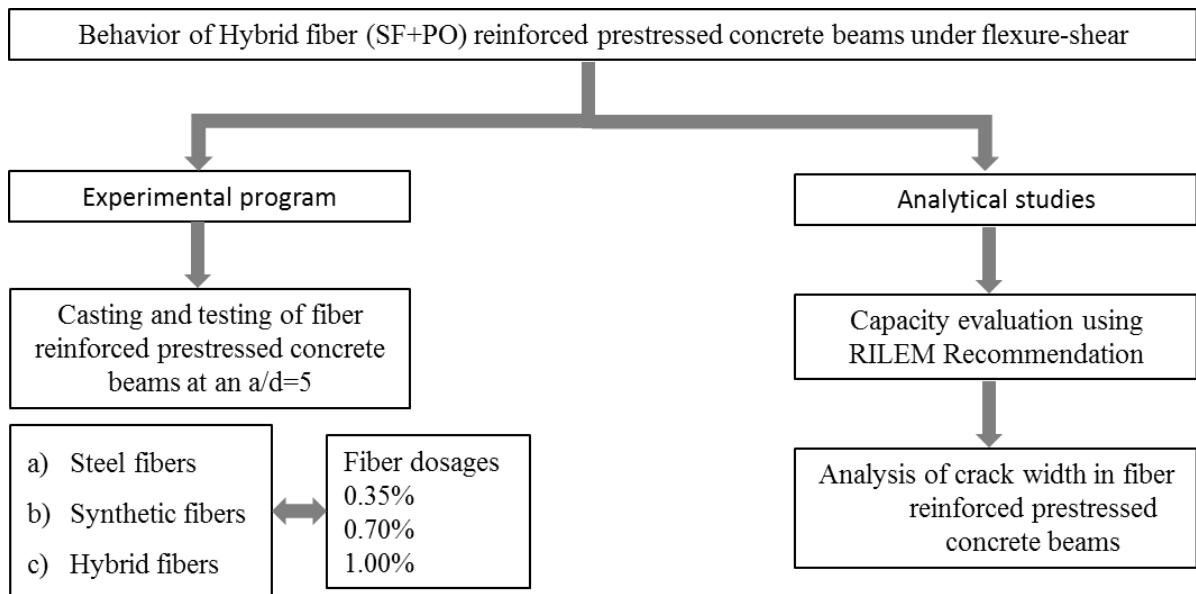


Figure 3.3: Workflow of the research plan

The scope of this work is limited to:

- 1) Casting and testing of full scale prestressed concrete beams with steel and synthetic fibers and a hybrid combination of both the fibers at various fiber dosages.
- 2) Understanding the flexure-shear behavior through load-displacement, load-strain (strand) response and failure modes of specimens.
- 3) Capacity calculation of prestressed fiber reinforced concrete beams using RILEM provisions and comparing the values with experimental results.
- 4) Crack width and crack spacing calculation using different models available in the literature.

Chapter 4

Experimental program



The experimental program consists of casting and testing of the full-scale prestressed concrete beams, having a length of 3.5 m and cross section 200 mm x 300 mm containing different fiber dosages, designed as per IS1343-2012 [29]. Four different series of beams corresponding to fiber dosages of 0, 0.35%, 0.70%, and 1.0% were cast. Two beams were tested at each fiber dosage to ensure the consistency of test results. All these beams were tested at a shear span to depth ratio (a/d) of five to ensure flexure/ flexure-shear behavior. A strain energy based ductility measurement was employed to study the influence of fibers. This work is a part of a larger research program on investigating the effect of various types of fibers and their combinations on the performance improvement of prestressed concrete beams under different a/d ratios. However, results about only $a/d = 5$ are only presented in this thesis.

4.1. Material properties

4.1.1. Fibers

The hooked end steel fibers and macro-synthetic polyolefin fibers were used in developing fiber reinforced concrete mixes. The physical and mechanical properties of the fibers used are presented in Table 4.1.

Table 4.1: Properties of Steel and macro-synthetic fibers

| Properties | Fiber Type | |
|------------------------|-----------------------------------------------------------------------------------|------------------------------------------------------------------------------------|
| | Steel (SF) fiber | Polyolefin (PO) fiber |
| |  |  |
| Specific gravity | 7.85 | 0.91 |
| Length (mm) | 30 | 50 |
| Diameter (mm) | 0.6 | 0.5 |
| Aspect ratio | 50 | 100 |
| Tensile strength (MPa) | 1000 | 618 |
| Elastic Modulus (MPa) | 200000 | 10000 |

4.1.2. Concrete

All specimens were cast in the precast plant using ready-mix concrete designed as per IS: 10262-2009 [30] to have a 28-day target compressive strength of 58 MPa, the details of mix design are presented in

Table 4.2. Blended coarse aggregates of size 10 mm and 20 mm along with fine aggregates were used to obtain a uniform mix. After the 28 days of water curing, concrete cubes were tested to evaluate the compressive strength of concrete, and the results are reported in Table 4.3. Concrete cylinders were tested (Figure 4.1a) to obtain the stress-strain curves with and without steel fibers. The addition of steel fibers was found to significantly improve the strength and stiffness degradation in the post-peak region with better ductility (Figure 4.1b). In the coming sections, the nomenclature used for different specimens are, 'Control' indicates the specimens

without any fibers/ plain concrete. For fiber reinforced specimens, (Fiber name) (fiber dosage (%)*100). For example, SF35 denotes steel fiber reinforced specimens with a 0.35% volume fraction. Similarly, HB70- hybrid fiber (SF+PO) reinforced specimen with 0.7% fiber dosage, and PO100- polyolefin (synthetic) fiber reinforced specimen with 1.0% fiber dosage.

Table 4.2: Mix design details

| Concrete | Quantities in kg/m ³ | | | | | | | | | |
|----------|---------------------------------|-------|-------|-------|-------|------|-------|--------------------------|----|----|
| | Aggregate | | | | C | F | W | Water reducing admixture | SF | PO |
| | 20 mm | 10 mm | CSS | NRS | | | | | | |
| Control | 754.0 | 355.0 | 415.0 | 313.0 | 428.0 | 22.0 | 165.0 | 2.5 | - | - |

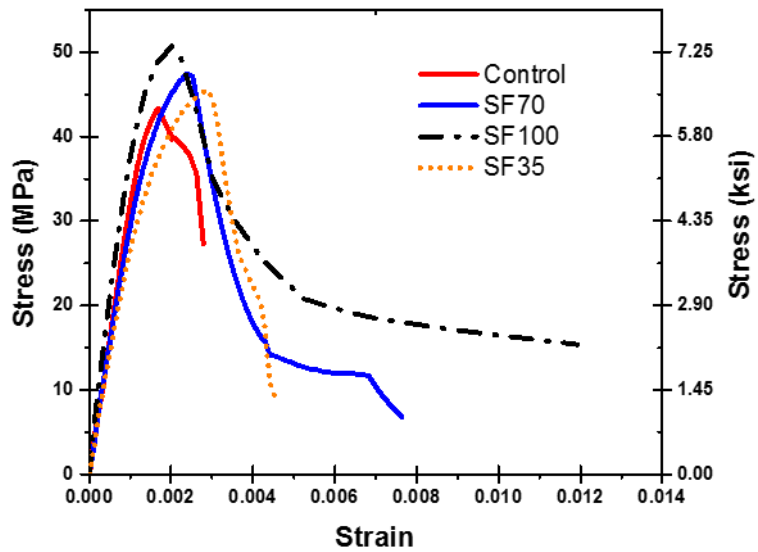
CSS - Crushed stone sand, NRS - Natural river sand, C – Cement, F – Flyash, W – Water, SF – Steel fiber, PO- Polyolefin fiber

Table 4.3: Details of concrete specimens

| Series | Dosage of fiber (%) | | Quantities in kg/m ³ | | Average cube strength(MPa) | Standard deviation(S D) in MPa |
|---------|---------------------|------------|---------------------------------|------|----------------------------|--------------------------------|
| | Steel | Polyolefin | SF | PO | | |
| Control | 0.000 | 0.000 | - | - | 65.00 | 2.42 |
| SF35 | 0.350 | 0.000 | 27.47 | - | 62.00 | 0.75 |
| PO35 | 0.000 | 0.350 | - | 3.18 | 67.00 | 2.82 |
| HB35 | 0.175 | 0.175 | 13.73 | 1.59 | 72.00 | 3.53 |
| SF70 | 0.700 | 0.000 | 54.94 | - | 61.00 | 0.15 |
| PO70 | 0.000 | 0.700 | - | 6.37 | 74.00 | 1.33 |
| HB70 | 0.350 | 0.350 | 27.47 | 3.18 | 63.00 | 2.24 |
| SF100 | 1.000 | 0.000 | 78.50 | - | 63.00 | 0.30 |
| PO100 | 0.000 | 1.000 | - | 9.10 | 72.00 | 2.05 |
| HB100 | 0.500 | 0.500 | 39.25 | 4.55 | 74.00 | 2.02 |



(a) Test Setup



(b) Stress strain curves Control vs. FRC

Figure 4.1: Cylinder testing under compression.

4.1.3. Internal reinforcement-prestressing steel strand

Two numbers of half an inch (12.7 mm diameter) strands containing seven low relaxation wires with an effective area of 200 mm² were used for prestressing the beams. Coupon specimens were prepared for tendons and tested under tension using a servo-controlled machine. The ultimate tensile strength and modulus of elasticity were found to be 1860 MPa and 196.5 GPa respectively. Jacking force is applied to each of the strands to subject them to an initial strain of 0.004.

4.2. Specimen preparation

Prestressed concrete beams of size 200 mm x 300 mm x 3500 mm were cast with an initial prestressing in the strand. Two numbers of seven wired low relaxations prestressing strand were used as longitudinal reinforcement. Strands were introduced at an eccentricity of 100 mm

throughout the length of the beam and were pre-tensioned to a strain of 0.004 (78.36 kN per each strand). All the test specimens were grouped into four different series namely control series (plain concrete without fibers), steel fiber (SF), macro-synthetic polyolefin (PO) and hybrid fiber (HB) reinforced series containing a combination of steel and macro-synthetic fibers. Moreover, the control specimens were designed to fail in flexure-shear mode. The process involved in the casting of fiber reinforced prestressed concrete beams is shown in Figure 4.2.



a) Mold preparation



b) Strand strain measurement during pretensioning



c) Placing of concrete



d) Compaction of concrete



e) cubes and cylinders

Figure 4.2: Casting process of fiber reinforced prestressed concrete beams

4.3. Test setup and Instrumentation

4.3.1. Fracture tests on fiber reinforced concrete specimens

Fracture tests were carried out to evaluate the performance of fiber reinforced concrete (FRC). The test setup consists of notched FRC prism (150mm x 150mm x 500mm) with a notch (5mm

width and 25mm depth), prepared as per the EN 14651-2005 [31] guidelines. The crack mouth opening displacement (CMOD) was measured using a clip gauge attached to the notch. CMOD is one of the main parameter used to evaluate the fracture behavior of fiber reinforced concrete specimens. All the fracture specimens were tested under three-point bending configuration (Figure 4.3). Displacement controlled loading was applied corresponding to the CMOD rate of 0.05mm/min. The fiber dosages in fracture tests were slightly different (0, 0.50%, 0.75%, 1.0%) than that used in the full-scale testing of prestressed beams (0, 0.35%, 0.70%, and 1.0%). Different dosages were considered in full-scale tests to evaluate the efficiency of very low (0.35%), medium (0.70%) and high (1.0%) fiber dosages. Nevertheless, fracture tests were intended to give an idea of the efficiency of hybrid fiber dosages before full-scale testing.

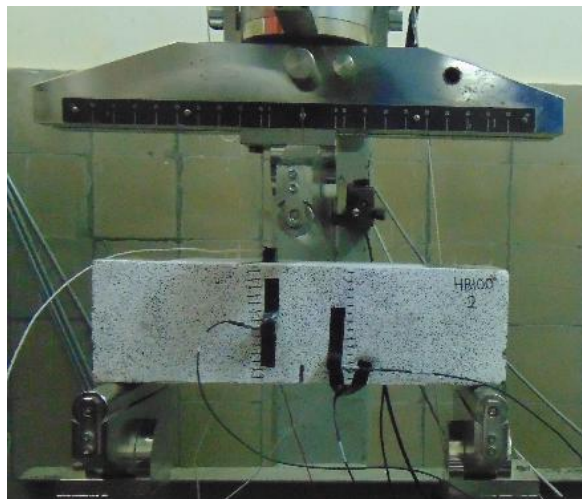


Figure 4.3: Fracture test setup

4.3.2. Full-scale tests on fiber reinforced prestressed concrete beams

In the present study, a/d ratio of five was chosen to investigate the effect of fiber hybridization (SF+PO) on flexure-shear behavior, and the response is compared to that of the specimens reinforced with only SF or PO fibers. All the specimens were simply supported and subjected

to two-point loading as shown in Figure 4.4. The horizontal movement of the support is restrained. Support width is expected to have minimal influence on the behavior as the specimens are tested at higher a/d ratio of 5.

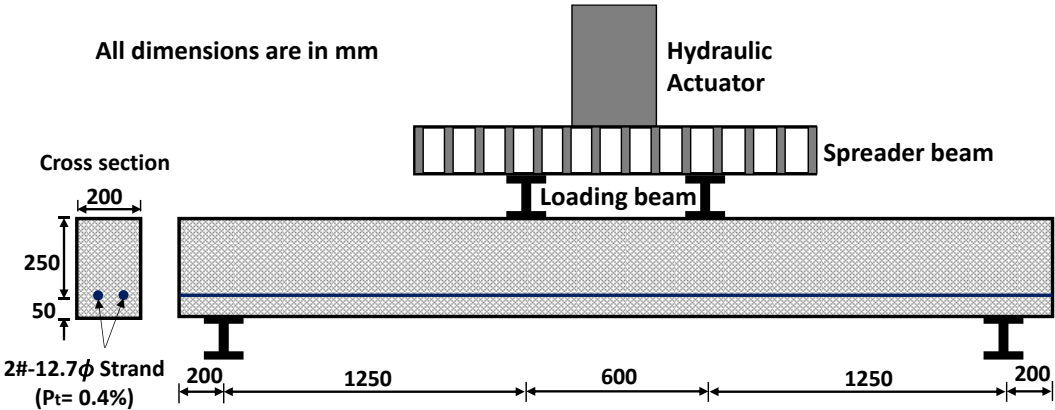
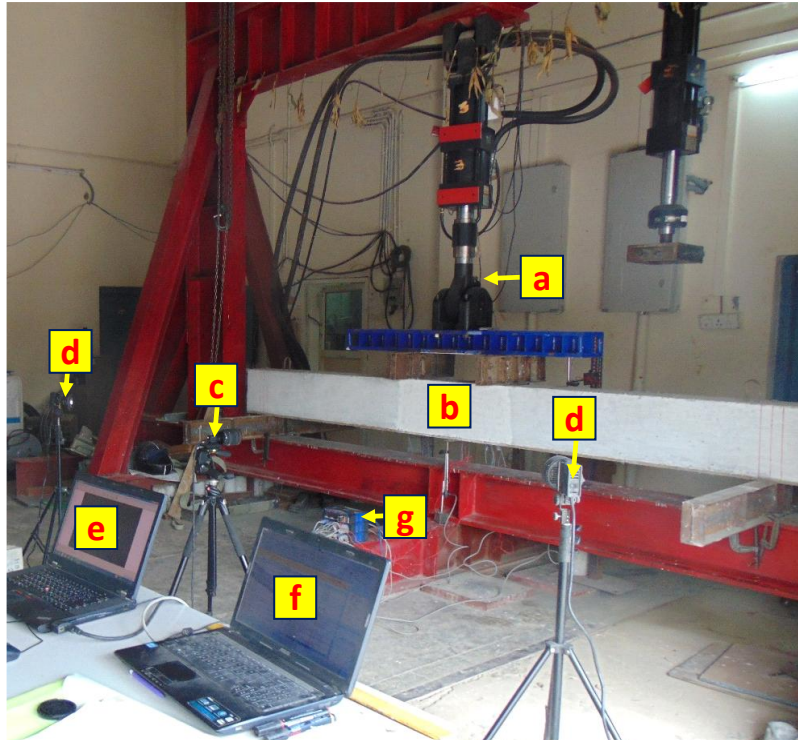


Figure 4.4: Schematic Details of the Test Specimen

The test setup and loading configuration are presented in Figure 4.5. MTS hydraulic actuator of 250 kN capacity was used for application of the static load. The static load was applied in displacement control, at a rate of 0.05 mm/sec. At every 10 kN increment in load, the test was paused to mark the crack propagation. Linear variable displacement transducers (LVDTs) were used to measure displacements at mid-span and one-third of the span. In total, four numbers of LVDTs are used to measure deflection at mid-span (2 numbers.) and third middle locations from support (2 numbers). Strain gauges were attached during the casting process to the prestressing strand at the mid-span to measure the strain variation during the load history. External data acquisition system (DAQ) was used to acquire data from various instruments during testing.



a. MTS Actuator (250kN); b. PSC Beam; c. Camera; d. Light source; e. MTS Controls system; f. DAQ Controller; g. DAQ system

Figure 4.5: Test setup and Instrumentations

4.3.3. Digital Image Correlation (DIC) technique

Digital image correlation (DIC) is a technique for measuring the whole-field strain and displacement of specimens. DIC works by comparing two images of the specimen coated with a random speckle pattern in an undeformed and deformed state (Schreier et al. [32]). Images of the object's surface before and after deformation are recorded, digitized and stored in the computer. These images are then analyzed to determine the displacements by invoking a pattern matching principle. Since it is impossible to find matching points using single pixel, areas (called as subsets) containing multiple pixels are used for the analysis. The size of the subset varies concerning the experimentation details. The step size controls the density of the analyzed data. For example, a step size of 5 will analyze every 5th point in each direction. A higher step size gives faster results but coarser data. A smaller step size will return more points but will

take more computation time. For the present experiments, a subset size of 35 and a step size of five was chosen after a thorough sensitivity analysis. All the specimens had a speckle pattern on the surface for capturing of DIC images. The surface was initially coated with non-reflective white paint, and then black speckle was sprayed on the white coat. Two halogen lights were placed at an angle to the specimen as shown in Figure 4.6 to illuminate the specimen. The camera was placed in front of the specimen with its axis is normal to the specimen. Images were taken at regular intervals and were processed using specialized software (VIC- 2D) for strain analysis, crack initiation and propagation.

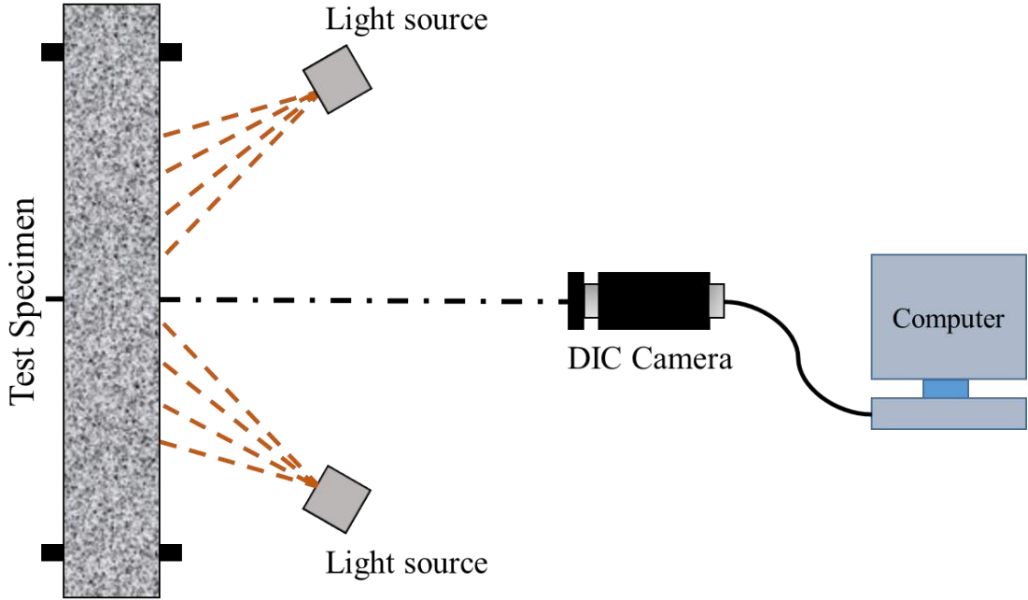


Figure 4.6: Schematic plan view of DIC setup

Chapter 5

Test results and Discussions

5.1. General

The experimental results of control, steel, polyolefin and hybrid fiber reinforced prestressed concrete under flexure-shear are presented in this chapter. All the beams are tested at shear span to depth ratio of five and the load vs. mid-span deflection plots are obtained. Two specimens were tested for each fiber dosage to ensure the consistency of the results. To understand the influence of different fibers at the material level, fracture behavior is also investigated and presented.

5.2. Fracture behavior of fiber reinforced concrete

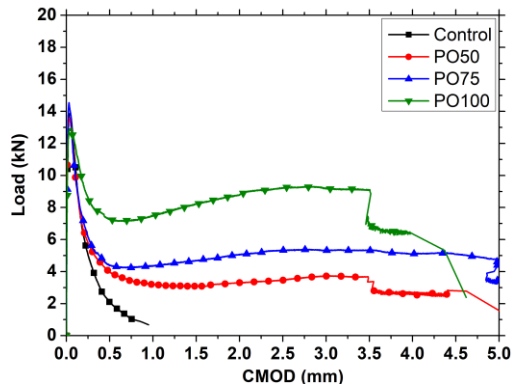
Fracture behavior is a multi-scale process, where each type of fiber can facilitate crack arresting at one strain level or within a limited range of strain. Therefore, to enhance the overall performance of FRC and to increase the effectiveness of fibers, the optimization of fiber dosage is essential for various fiber types and combinations. SFRC has been found to show better performance within small crack mouth opening displacement (CMOD) values with a quick load recovery after the cracking. However, the load drop is significant for the synthetic fiber reinforced concrete (SynFRC) after first cracking. Load resistance in SynFRC occurred at the higher values of CMOD. The difference in the performance of these fibers is due to the elastic stiffness of fibers, adhesion with concrete and other geometrical properties of the fibers.

Therefore, understanding the fracture behavior of hybrid fiber reinforced concrete (HFRC) is essential for its inclusion in structural design. Fracture tests were conducted to evaluate the efficiency of different fibers. The results of the load vs. crack mouth opening displacement (CMOD) of SynFRC, SFRC, and HFRC (SF+PO) are presented in Figure 5.1. From load vs. CMOD graphs, it can be inferred that steel fibers restrict the crack opening better than polyolefin fibers. Usage of hybrid fiber combination tends to shift the curve towards that of the steel fiber reinforced specimen, indicating better synergy between steel and synthetic fibers.

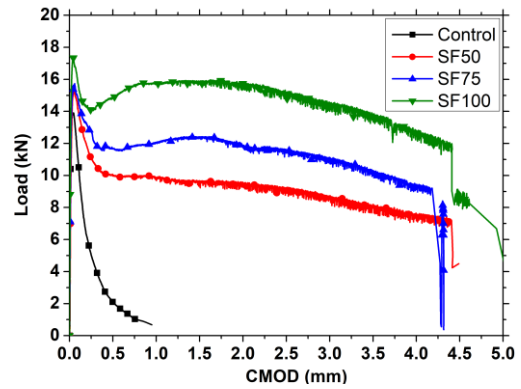
A hybrid combination of steel and synthetic fibers as additional secondary reinforcements could improve both the fracture resistance and the toughness. The load vs. CMOD curves (Figure 5.1a-c) show the ability of hybrid fibers in crack arresting. Figure 5.1 also shows that the synergetic reinforcing outcomes of steel and synthetic fibers are noticeable. The synergy is because of the addition of fibers having different mechanical properties and aspect ratios (Length/Diameter) and their roles at a micro/macro level to enhance the strength and stiffness of concrete. However, due to the superior mechanical properties of steel fibers, the SFRC exhibits a lesser load drop soon-after cracking when compared to other fibers. The residual strength (f_R) of FRC is calculated at different CMOD values (0.5mm, 2.5mm, 3.5mm) using the equation (1) as per EN 14651-2005 [31] standards. The residual strength calculated is summarized in Table 5.1. Due to the longer interface length between the concrete matrix and PO fiber, SynFRC specimens are shown to exhibit significant residual strength at higher CMODs (Table 5.1).

$$f_{R,j} = \frac{1.5(F_{R,j})L}{D(D_{lig})^2} \quad - (5.1)$$

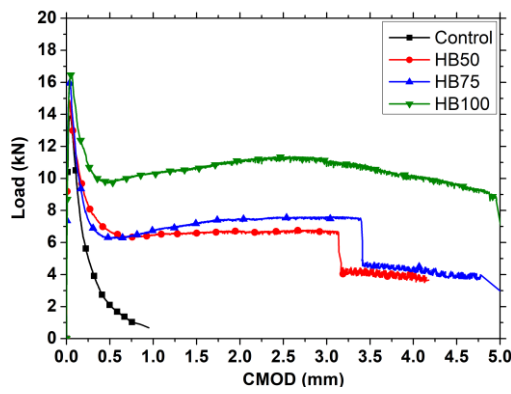
Where $f_{R,j}$ = j^{th} residual strength; $F_{R,j}$ = j^{th} residual load; L= span; D= depth of beam; D_{lig} = depth of ligament.



(a) SynFRC (PO)



(b) SFRC (SF)



(c) HFRC (SF+PO)

Figure 5.1: Typical Load Vs. CMOD Curves of FRC [3]

Table 5.1: Residual flexural strength of FRC specimens

| Specimen | CMOD | | |
|----------|----------------|----------------|----------------|
| | 0.5mm | 2.5mm | 3.5mm |
| | f_{R1} (MPa) | f_{R3} (MPa) | f_{R4} (MPa) |
| Control | 0.60 | -- | -- |
| PO50 | 1.14 | 1.00 | 0.96 |
| PO75 | 1.26 | 1.53 | 1.53 |
| PO100 | 2.09 | 2.66 | 2.61 |
| SF50 | 2.89 | 2.66 | 2.35 |
| SF75 | 3.36 | 3.34 | 2.97 |
| SF100 | 4.27 | 4.34 | 3.99 |
| HB50 | 1.93 | 1.93 | 1.15 |
| HB75 | 1.94 | 2.05 | 1.87 |
| HB100 | 2.81 | 3.27 | 3.09 |

5.1. Full-scale testing of prestressed concrete specimens without fibers (Control specimen)

In control specimens, the initial cracks formed at a load of 60 kN. After the initial cracking, the stiffness of the specimen reduced due to the formation and propagation of multiple cracks. Finally, after reaching an ultimate load (130 kN), the specimen abruptly failed in flexure-shear mode, which was catastrophic. It is worth mentioning that the beam was heavily under reinforced leading to the yielding of strands just before the peak load, on further increase in loads, flexural crack converted to shear and propagated through aggregates leading to sudden energy release at failure. The flexure-shear failure mode of a control specimen is presented in Figure 5.3. In this study, if the final failure of the beam is due to shear tension cracking after the yielding of the prestressing strand, it is defined as the flexure-shear mode. Three control specimens were tested, out of which behavior control-2 was in the range between control-1 and control-3. Hence control-2 has considered for further comparison with other fiber reinforced specimens, and control-2 is termed as control specimen in all other graphs.

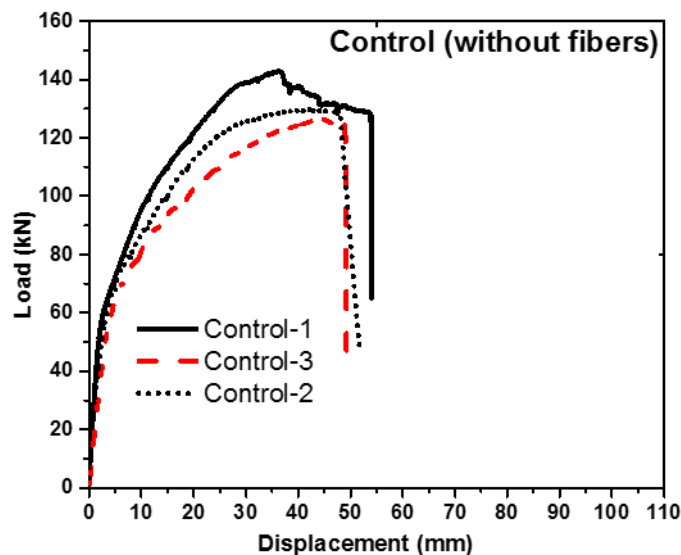
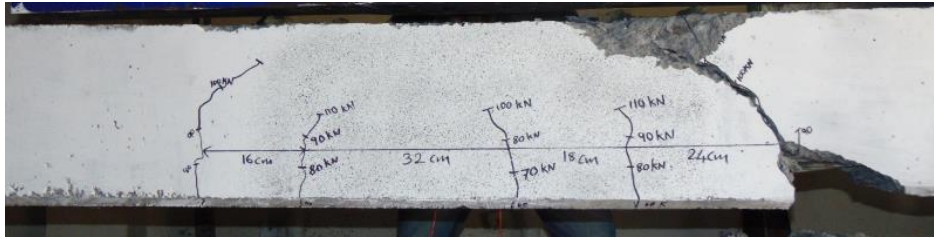
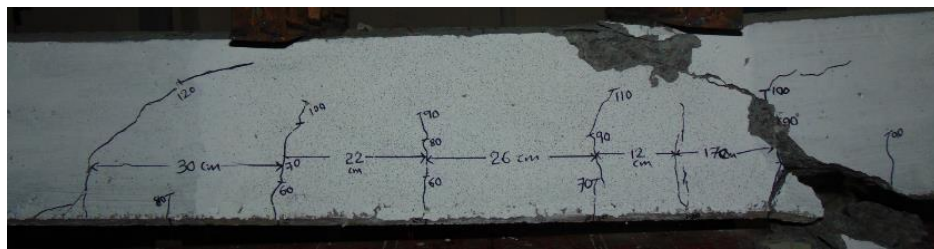


Figure 5.2: Behavior of control specimen (without fibers)



a) The failure mode of the PO00-1 specimen



b) The failure mode of the PO00-2 specimen



c) The failure mode of the SF00-1 specimen

Figure 5.3: Flexure-shear failure of control specimens

5.2. The behavior of Steel fiber reinforced prestressed concrete specimens

5.2.1. Specimens with 0.35% dosage of steel fibers

The beams with 0.35% of steel fibers exhibited better ductility as compared to the control specimen. About 13% improvement in cracking load and 23% (average) improvement in post-cracking stiffness was observed (Figure 5.4). However, the ultimate load did not change. SF35 series of beams had better crack distribution with the delayed formation of cracks as compared to the control specimen before reaching its final failure load. Flexure dominant failure (Figure 5.5) was observed with 0.35% steel fiber dosage. The crack bridging effect was evident through the formation of a number of smaller cracks and fewer major cracks.

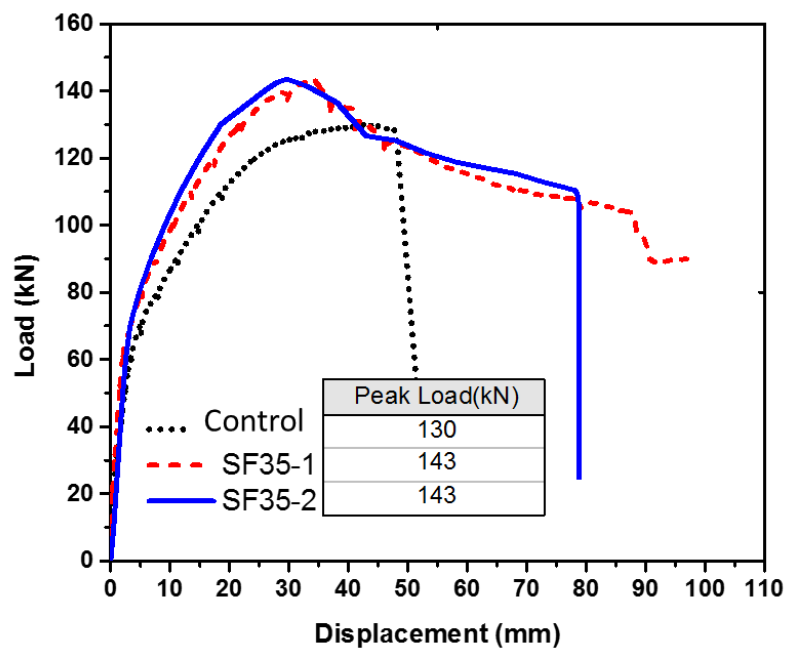


Figure 5.4: Behavior of 0.35% dosage of steel fiber reinforced specimens



Figure 5.5: Flexure failure of SF35 specimen

5.2.2. Specimens with 0.70% dosage of steel fibers

The specimen with 0.7% steel fiber dosage (Figure 5.6) exhibited better ductility than the specimen with a 0.35% fiber dosage. However, there was no substantial improvement in the ultimate strength due to the higher fiber dosage. The presence of steel fibers resulted in more distribution of cracks, and gradual ductile failure (Figure 5.7) mode was observed. Due to a limitation in stroke capacity of the actuator, the test was terminated when the actuator displacement reached the vicinity of 100 mm. The average capacity (peak load) of the SF70 specimen is 147 kN.

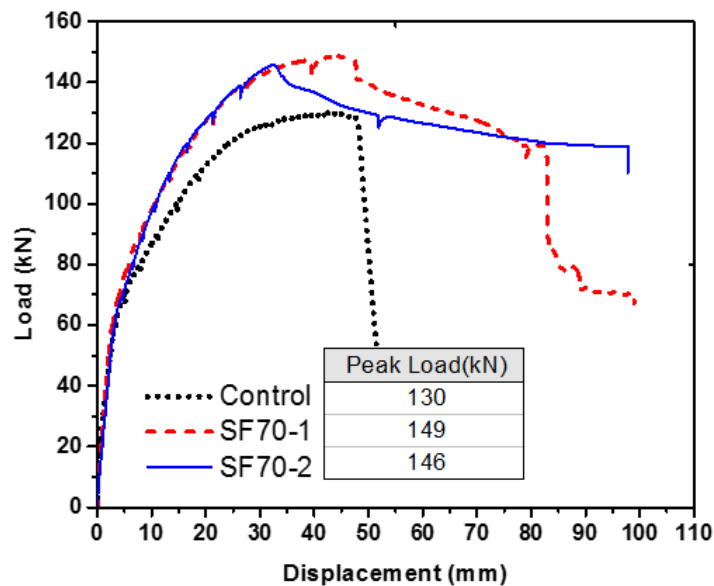


Figure 5.6: Behavior of 0.7% dosage of steel fiber reinforced specimens

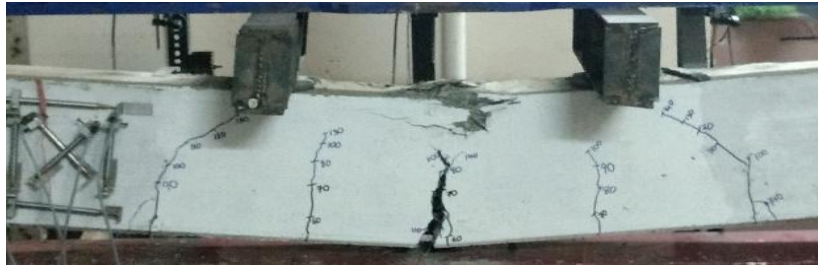


Figure 5.7: Flexure failure of SF70 specimen

5.2.3. Specimens with 1.0% dosage of steel fibers

Significant improvement in the post-cracking stiffness (50%), ductility and ultimate load (11.6%) were observed with the increase in fiber dosage from 0% to 1.0%. The specimen had an ultimate load of 159 kN with the first crack forming at a load of 70 kN. The test was terminated at 100 mm displacement due to a limitation in stroke capacity of the actuator. However, the specimen could have resisted loads at even higher displacements which is evident from the overall load-displacement curves (Figure 5.8). It was evident from the test results that the presence of steel fiber increases the displacement corresponding to the cracking load. The addition of fibers also converted the brittle flexure-shear failure of control beams into ductile flexure dominant failure in fiber reinforced beams (Figure 5.9). One specimen with 1.0% steel fiber dosage had honeycombing due to improper compaction, and hence it was excluded from comparisons.

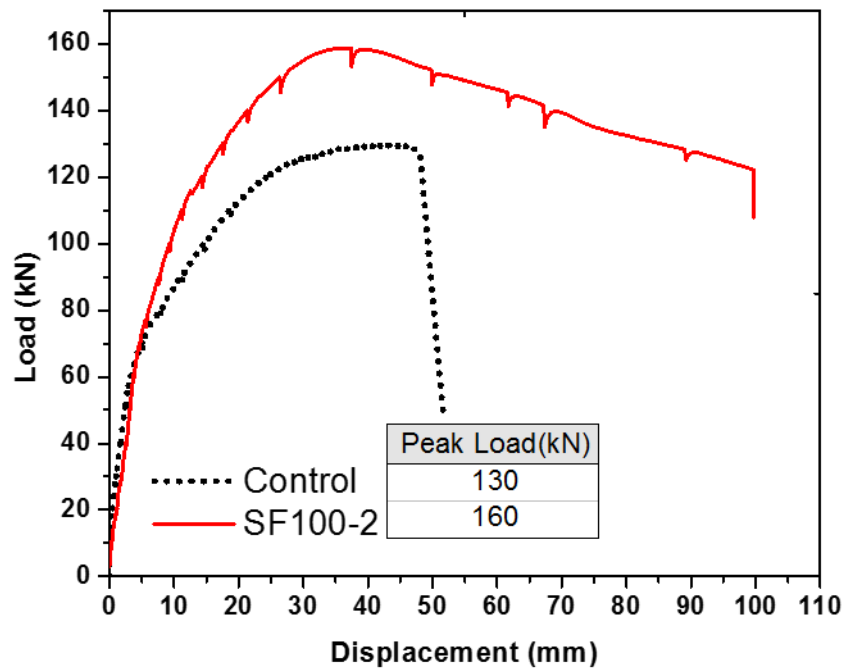


Figure 5.8: Behavior of 1.0% dosage of steel fiber reinforced specimens

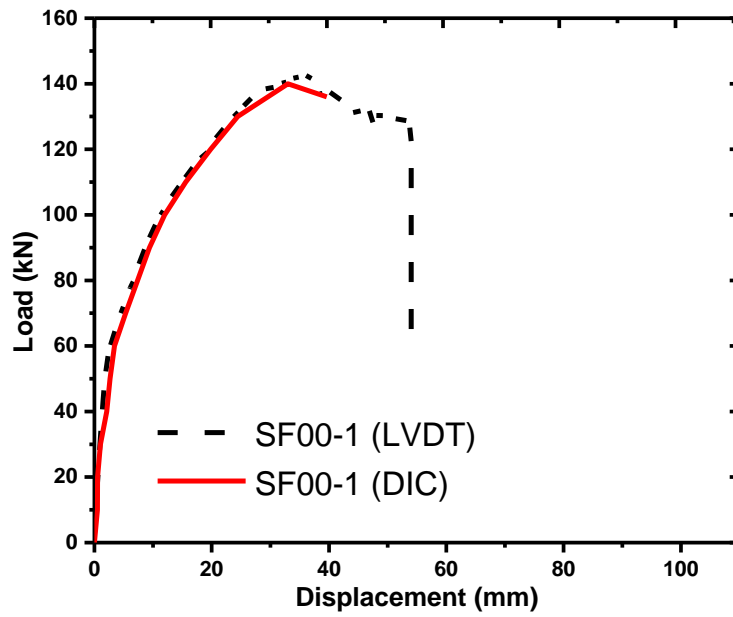


Figure 5.9: Flexure failure of SF100 specimen

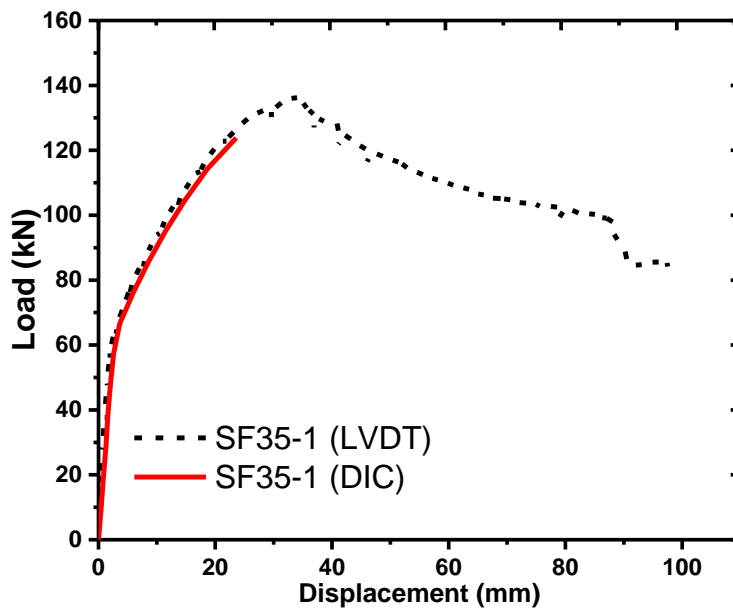
5.2.4. Analysis of results using digital image correlation

Load vs. deflection analysis: Displacements and strains from DIC analysis can be correlated only until major crack formation. After significant cracking, the correlation breaks due to excessive cracking and spalling of concrete leading to the difficulty in pattern matching. The load-deflection response of the specimens using DIC analysis is compared with the LVDT

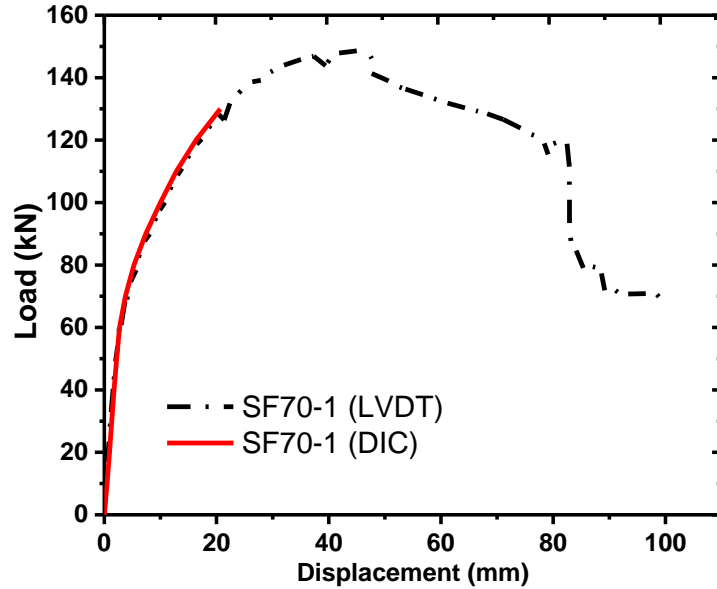
measurements for beams with different fiber dosages (Figure 5.10). The results from DIC analysis showed a close agreement with the LVDT measurements.



a) Control specimen (DIC)



b) Prestressed concrete beams with 0.35% steel fibers (DIC)

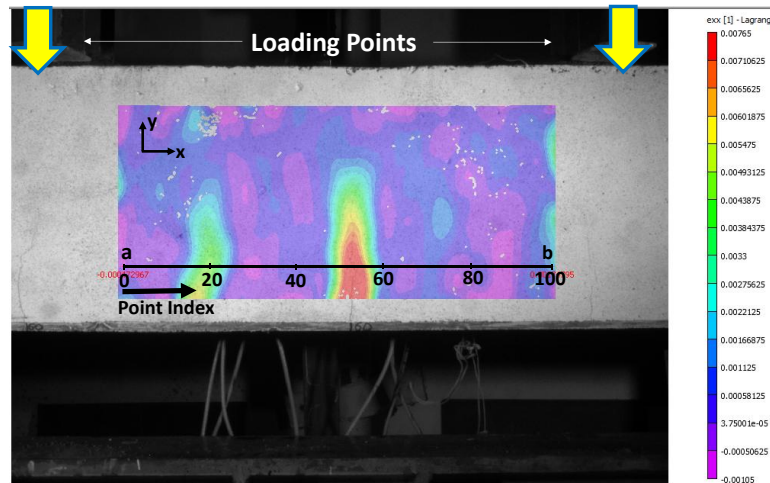


b) Prestressed concrete beams with 0.70% steel fibers (DIC)

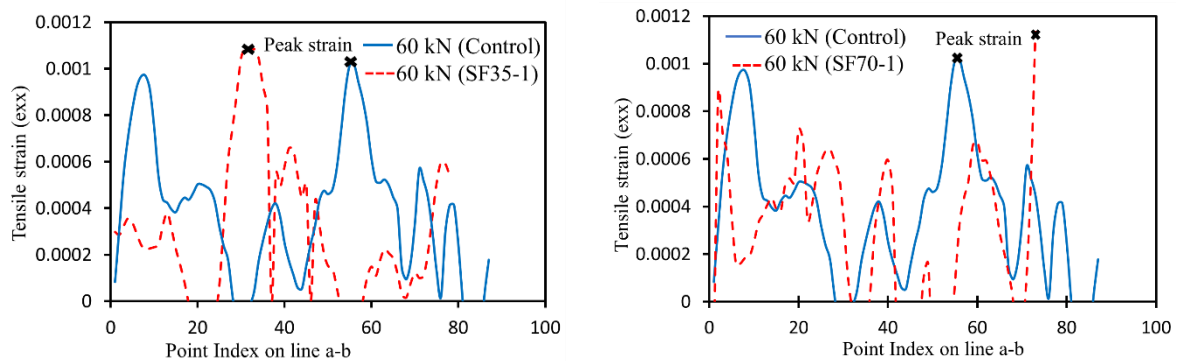
Figure 5.10: Deflection measurements from DIC analysis and compared with LVDT readings

Effect of steel fibers on the tensile strain in the concrete: Full field strains on the surfaces were measured using the VIC-2D software. Strain distribution was evaluated to see the effect of steel fiber contribution in resisting the crack propagation. A horizontal line a-b was chosen (Figure 5.11a) in the tensile zone of all the tested beams. Figure 5.11b shows the tensile strain variation along the line a-b at a load level of 60 kN, which is slightly less than the cracking load. It indicates that the peak strain along the considered horizontal line is the same for beams of different series. This elucidates the fact that fibers do not play a vital role in load carrying mechanisms before cracking. On the other hand, Figure 5.11c shows the tensile strain variation along line a-b at a load of 70 kN, which is greater than the cracking load. It presents the decrease in peak strain at the same load level after cracking with the increase in fiber dosage. The reduction in strain indicates that fibers resist the crack widening, localization and helps to redistribute the stresses and increase the number of cracks. The extent of reduction in strains

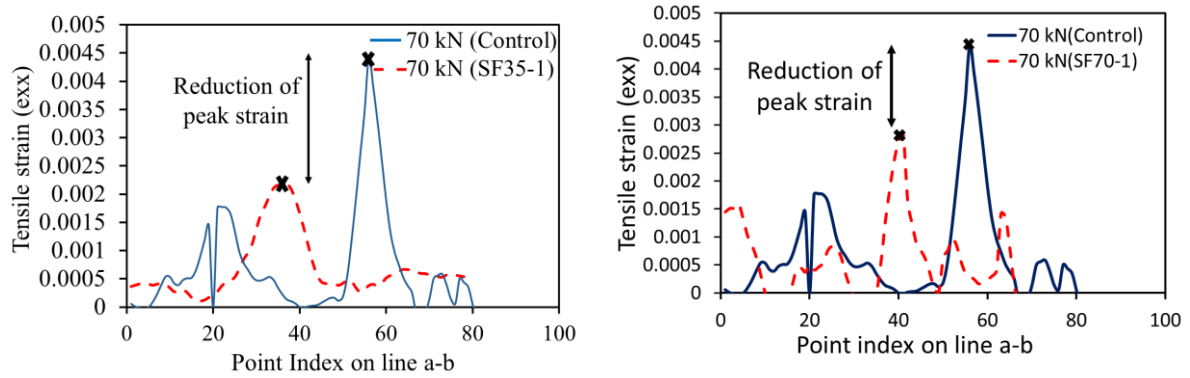
mainly depends on the dosage of steel fibers. In Figure 5.11a-c, a sudden jump in the strain contour indicates the presence of a crack in that region. Figure 5.12 illustrates the reduction in average strain along the level of the crack tip at failure due to the addition of fiber. Additionally, Figure 5.11 also indicates that the presence of steel fiber reduces the maximum strain as much as 50%. The strain values corresponding to the post-cracking loads for different specimen highlights that the presence of steel fibers reduces the strain at the crack locations (Figure 5.12). DIC results pertaining to only steel fiber reinforced specimens were presented in this thesis, as the DIC results of PO and HB series were inconsistent due to a) correlation problem b) actual failure crack was not captured within the area of interest.



a) Horizontal line a-b in the tension zone for Analysis (Constant Moment Zone)



b) Tensile Strain at 60 kN (before cracking)



c) Tensile Strain at 70 kN (after cracking)

Figure 5.11: Longitudinal strain contours (DIC) on the horizontal line a-b before and after cracking

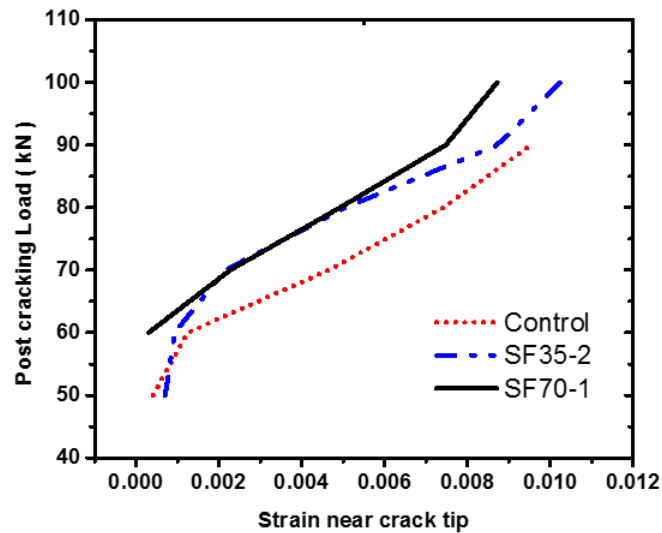


Figure 5.12: Average Strain along the level of the crack tip at failure

5.3. The behavior of Synthetic fiber reinforced prestressed concrete specimens

5.3.1. Specimens with 0.35% dosage of polyolefin fibers

Figure 5.13 shows the load-displacement behavior of beams with 0.35% fiber dosage of polyolefin fibers. Both the control and synthetic fiber reinforced specimens (PO-35) cracked at 60 kN. However, there was a slight improvement in the displacement ductility of the PO35 specimen. 0.35% dosage of synthetic fibers reinforced specimens (PO35) failed in flexure-

shear mode (Figure 5.14), as the final failure of the beam is due to shear tension cracking after the yielding of prestressing strand.

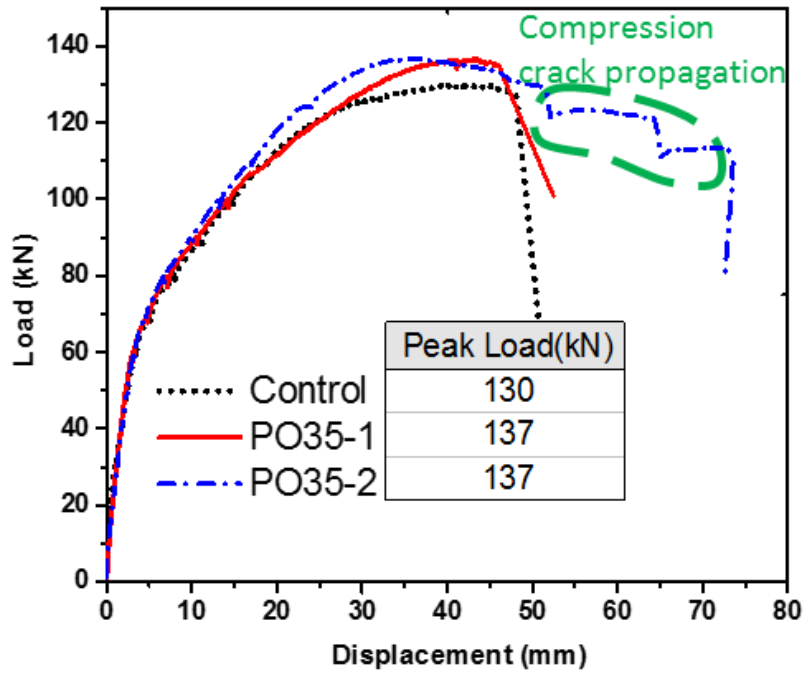
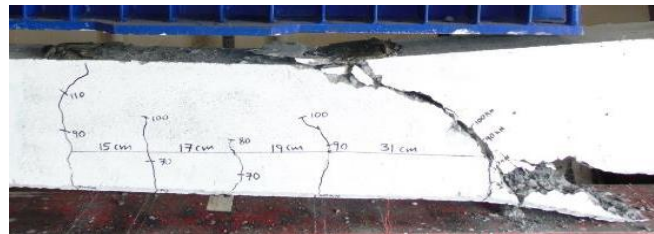
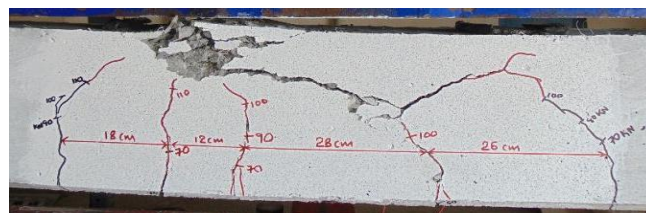


Figure 5.13: Behavior of 0.35% dosage of polyolefin fiber reinforced specimens



a) PO35-1 Specimen



b) PO35-2 Specimen

Figure 5.14: Flexure-shear failure of PO35 specimen

5.3.2. Specimens with 0.70% dosage of polyolefin fibers

When 0.7% of polyolefin fibers were added to the PSC members, post-cracking stiffness increased in fiber-reinforced beams as compared to post cracking stiffness of control specimen (Figure 5.15). This increase in stiffness is mainly due to the contribution of fibers in crack bridging. Though the diagonal shear cracks formed in PO specimens (0.70%), the fibers were effective in arresting the propagation of shear cracks, which resulted in the formation of flexural cracks (Figure 5.16). Due to a limitation in stroke capacity of the actuator, the test was terminated when the actuator displacement reached the vicinity of 100 mm (for both PO70 specimens). The cracking load (60 kN) did not change due to fiber addition; steel fibers influenced the cracking load as well.

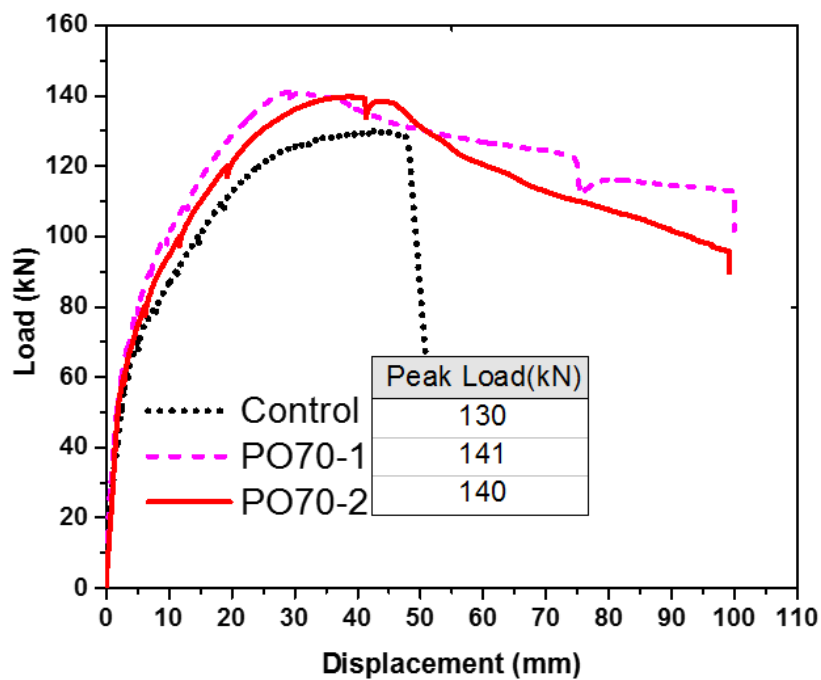
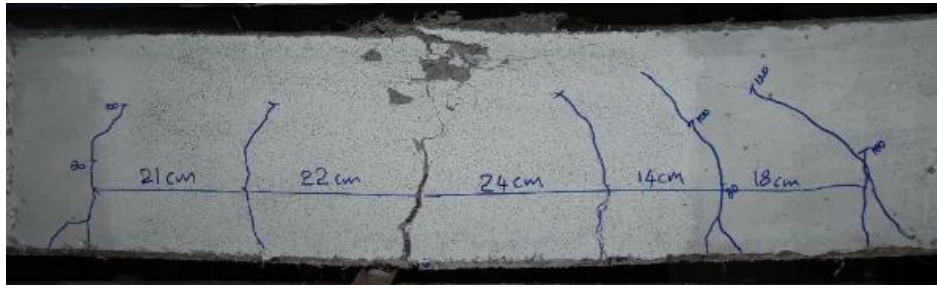


Figure 5.15: Behavior of 0.70% dosage of polyolefin fiber reinforced specimens



a) Well distributed flexure cracks



b) crack bridging action of PO fibers

Figure 5.16: Flexure behavior of PO70 specimen

5.3.3. Specimens with 1.00% dosage of polyolefin fibers

In case of beams with 1.0% polyolefin fiber dosage, the cracking load is not influenced by fiber addition and is found to be the same as that of the control specimen. Soon after cracking, there was a slight improvement in the post-cracking stiffness. However, the behavior is similar to that of control specimen up to peak load (Figure 5.17). After peak load (135 kN), the specimen continued to deform in an inelastic manner with a small load drop. It is observed that the polyolefin fibers arrested shear cracks and the two major flexural cracks continued to grow towards the top surface. Finally, dominant flexural behavior was observed (Figure 5.18). The testing was terminated for PO100-1 when the mid-span deflection reached 100 mm due to a limitation in the stroke capacity of the actuator. Also, one of the PO100 specimens had an instrumentation error and hence is not used for comparison of load-displacement curves.

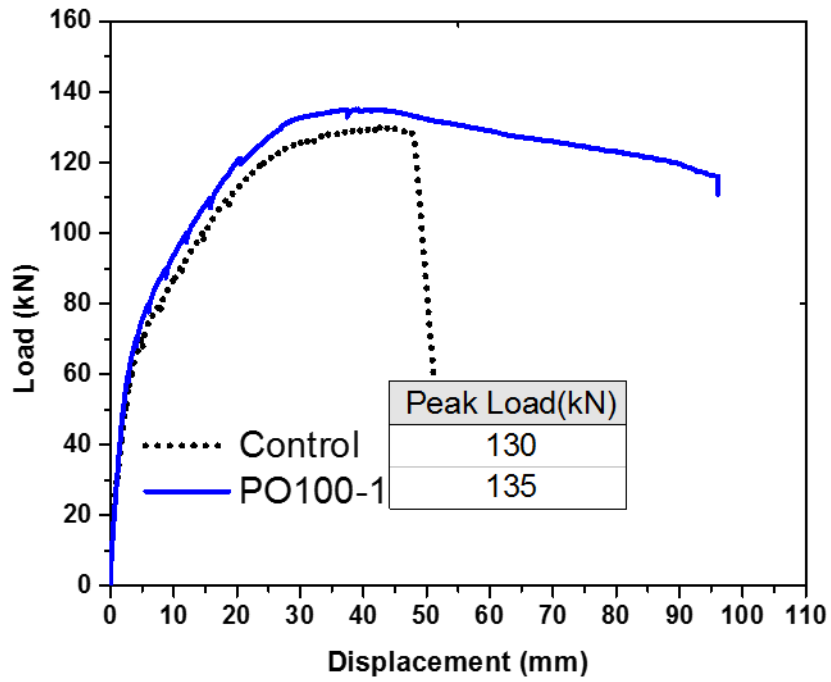
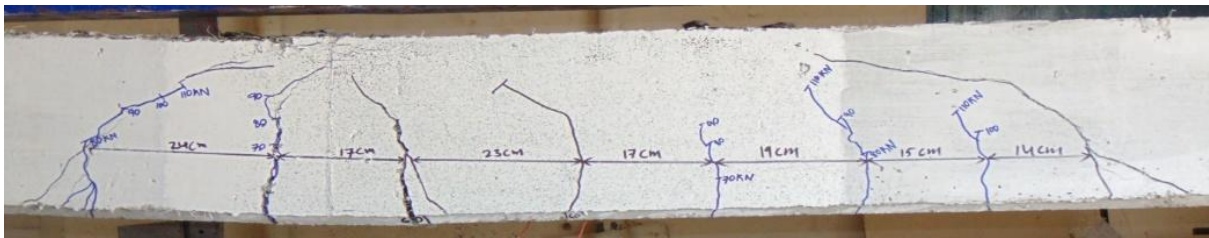


Figure 5.17: Behavior of 1.0% dosage of polyolefin fiber reinforced specimens



a) Flexure behavior resulted from arresting shear cracks of PO70 specimen



b) at major flexural crack location

Figure 5.18: Flexure behavior of PO100 specimen

5.4. Effect of hybridization of steel and synthetic fibers on flexure-shear behavior

5.4.1. Specimens with 0.35% dosage of hybrid fibers

When hybrid fiber (SF+PO) of 0.35% dosage is added to the concrete, cracking load increased by 25% (75 kN) (Figure 5.19). After cracking, specimen continued to resist the applied load by tension contribution of prestressing steel and passive contribution of the fibers at the cracked section. The average ultimate load of HB35 specimens is found to be 151.2 kN. It can be observed from Figure 5.19 that the HB35 specimens had an improved response compared to control specimens, even in the post-peak zone. Although new cracks did not form after the ultimate load, there was a drop-in load and gradual declination of the slope in the load-displacement curve due to the crack branching and propagation of the existing cracks. The flexure-shear crack was arrested by the fiber bridging action, and the final failure of the beam was in flexure mode (ductile) as shown in Figure 5.20. The final displacement at the failure was 80 mm.

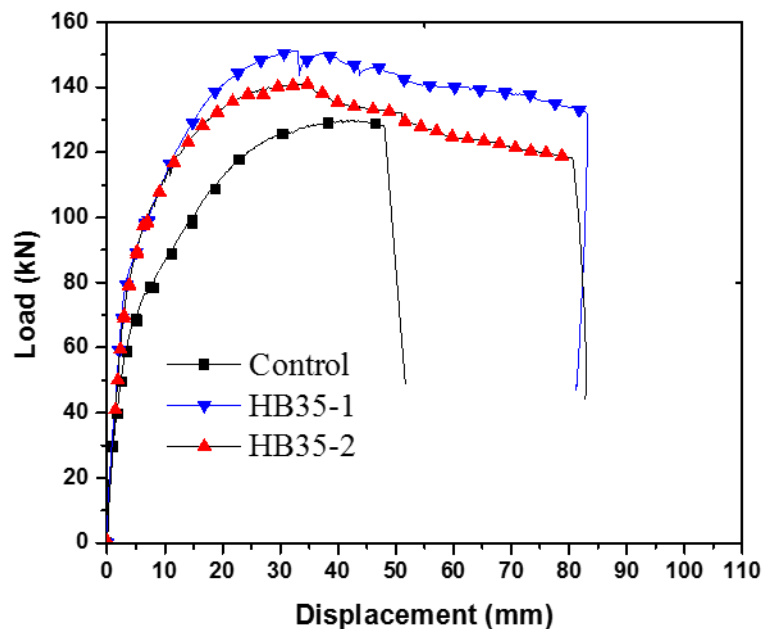


Figure 5.19: Behavior of 0.35% dosage of hybrid(SF+PO) fiber reinforced specimens



Figure 5.20: Flexure behavior of HB35 specimen

5.4.2. Specimens with 0.70% dosage of hybrid fibers

Figure 5.21 shows the behavior of the specimens reinforced with a 0.7% dosage of hybrid fibers. The average cracking load and ultimate load are observed to be 80 kN and 145.6 kN, respectively. Both the specimens of HB70 failed in ductile flexure mode (Figure 5.22) at the displacement of 80mm.

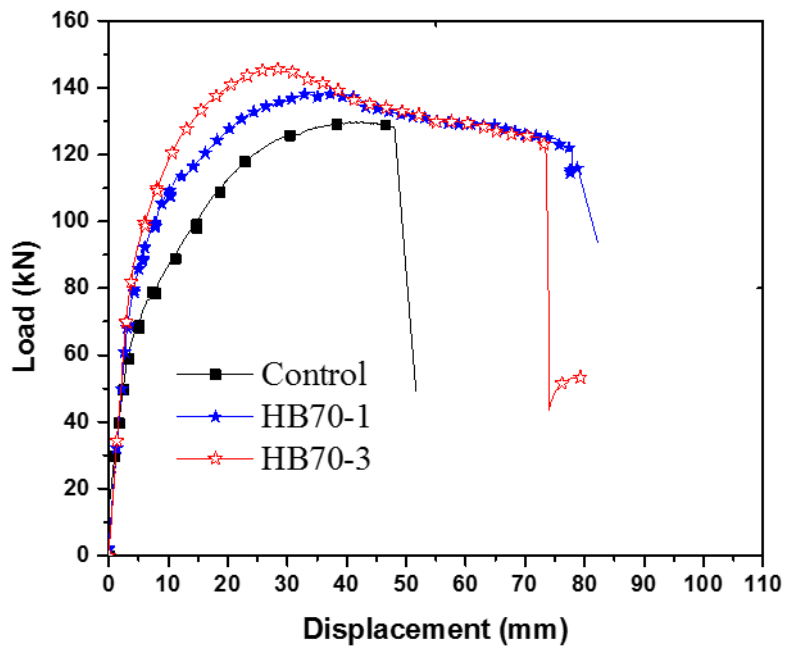


Figure 5.21: Behavior of 0.70% dosage of hybrid(SF+PO) fiber reinforced specimens

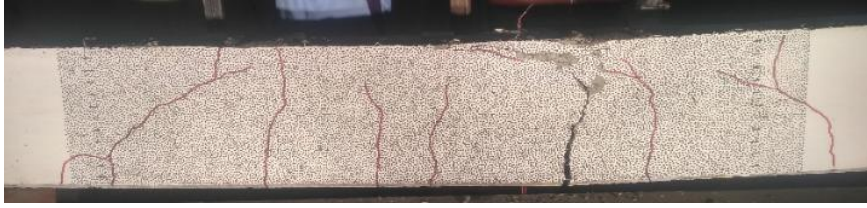


Figure 5.22: Flexure behavior of HB70 specimen

5.4.3. Specimens with 1.00% dosage of hybrid fibers

Flexure dominant behavior (Figure 5.23) was observed for 1.0% hybrid fiber reinforced specimens (cracking load = 80 kN and ultimate load = 141.7 kN). Compared to HB35 and HB70, specimens with 1.0% hybrid fibers exhibited better ductility (Figure 5.24) (ultimate displacement = 96 mm).

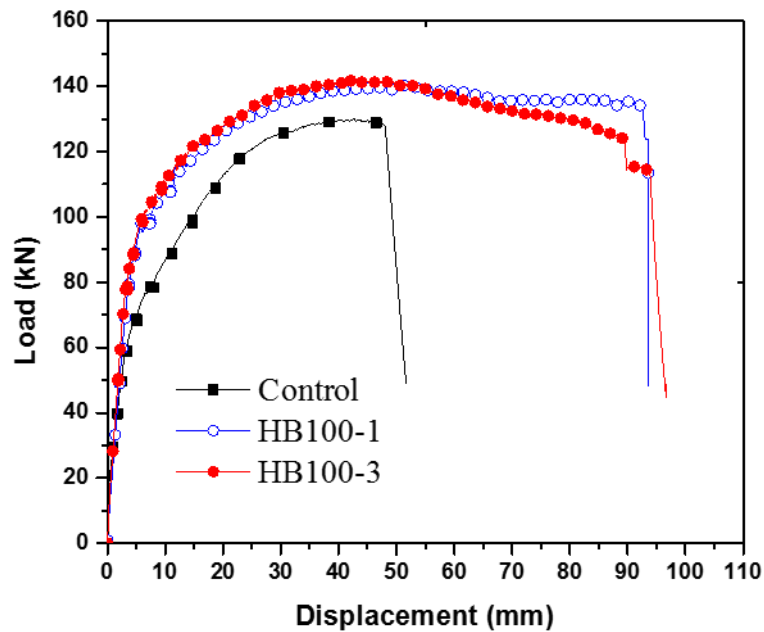


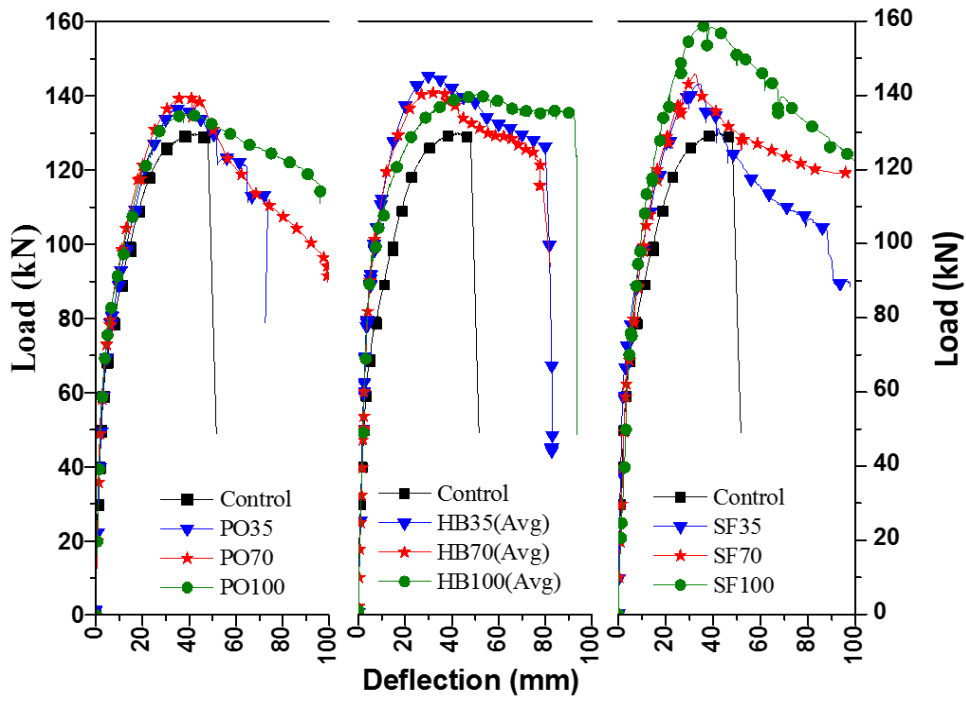
Figure 5.23: Behavior of 1.0% dosage of hybrid(SF+PO) fiber reinforced specimens



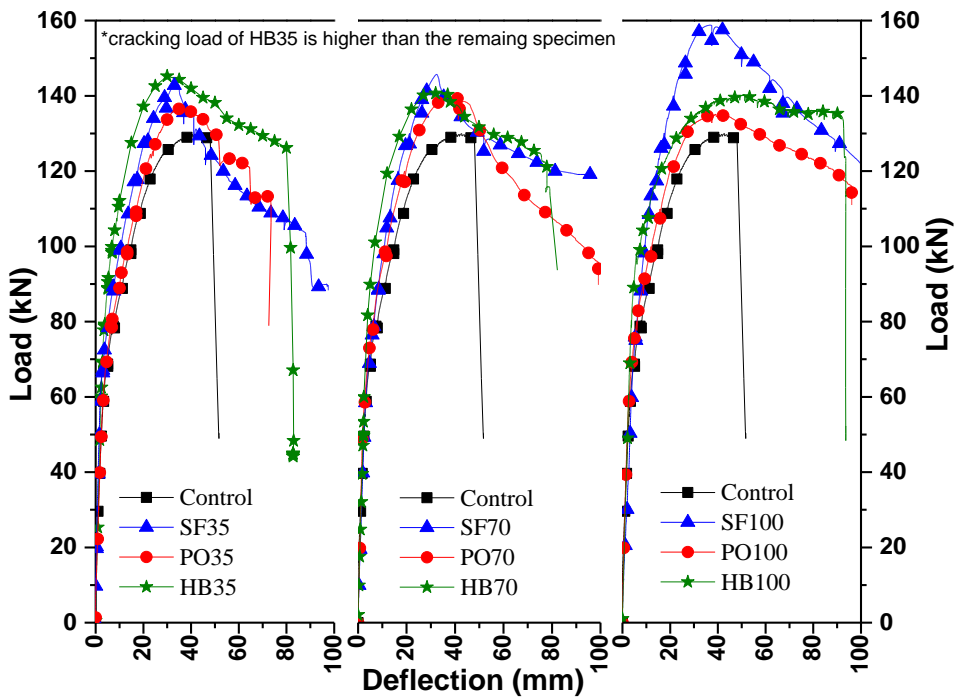
Figure 5.24: Flexure behavior of HB100 specimen

5.5. Behavior comparison of fiber reinforced prestressed concrete specimens

The behavior comparison of different fiber reinforced specimen viz. steel, synthetic and hybrid fibers at different fiber dosages are shown in Figure 5.25a. The effect of hybridization of steel and synthetic fibers compared to that of specimens reinforced with individual fiber are shown in Figure 5.25b. In the series of hybrid fiber reinforced specimens cracking load is higher than that of other series (SF, PO). In the case of specimens with 0.35% fibers, even though post cracking stiffness of SF35 and HB35 is similar and more than PO35 (Figure 5.25b), HB35 specimens failed at an early displacement compared to that of SF35. Moreover, the energy absorption capacity of HB35 and SF35 are comparable. The hybrid specimen (HB70) with 0.7% fiber dosage (Figure 5.25b) failed at a displacement of 80 mm whereas the specimen SF70 exhibited higher ductility. Even though SF70 specimen can undergo more plastic deformation, the testing of specimen SF70 was terminated at a displacement of 100 mm due to a limitation in actuator stroke capacity. Similarly, testing of PO70 specimen was terminated at an ultimate displacement of 100mm. At 1.0% fiber dosage, even though all the fiber reinforced specimen failed in flexure mode, the energy absorption capacity of SF specimens is higher than HB and PO. Overall, to conclude, the performance of prestressed specimens with steel fibers was better than that of hybrid and synthetic fibers.



a) The behavior of hybrid, steel, and synthetic FRC



(b) Behavior comparison of different FRC at same fiber dosages

Figure 5.25: Load-deflection behavior of fiber reinforced prestressed concrete beams

5.5.1. Crack pattern and failure mode comparison

Change in crack pattern and failure mode of the prestressed concrete beams due to fiber addition can be used to evaluate the effectiveness of different fibers. Control specimen had initial flexural cracks between the loading points. Finally, a shear crack propagated from previously formed flexure crack at the peak load and failed in a brittle mode. The control beam (without fibers) failed in flexure-shear mode (Figure 5.26a). When the fibers at a volume fraction of 0.35% were added to the concrete, HB35 and SF35 specimen arrested the shear crack propagation, and the final failure was in ductile flexure mode (Figure 5.26b, d). However, the number of fibers in PO35 could not completely arrest the propagation of the shear crack due to which the beam failed in a flexure-shear mode like the control beam (Figure 5.26c).

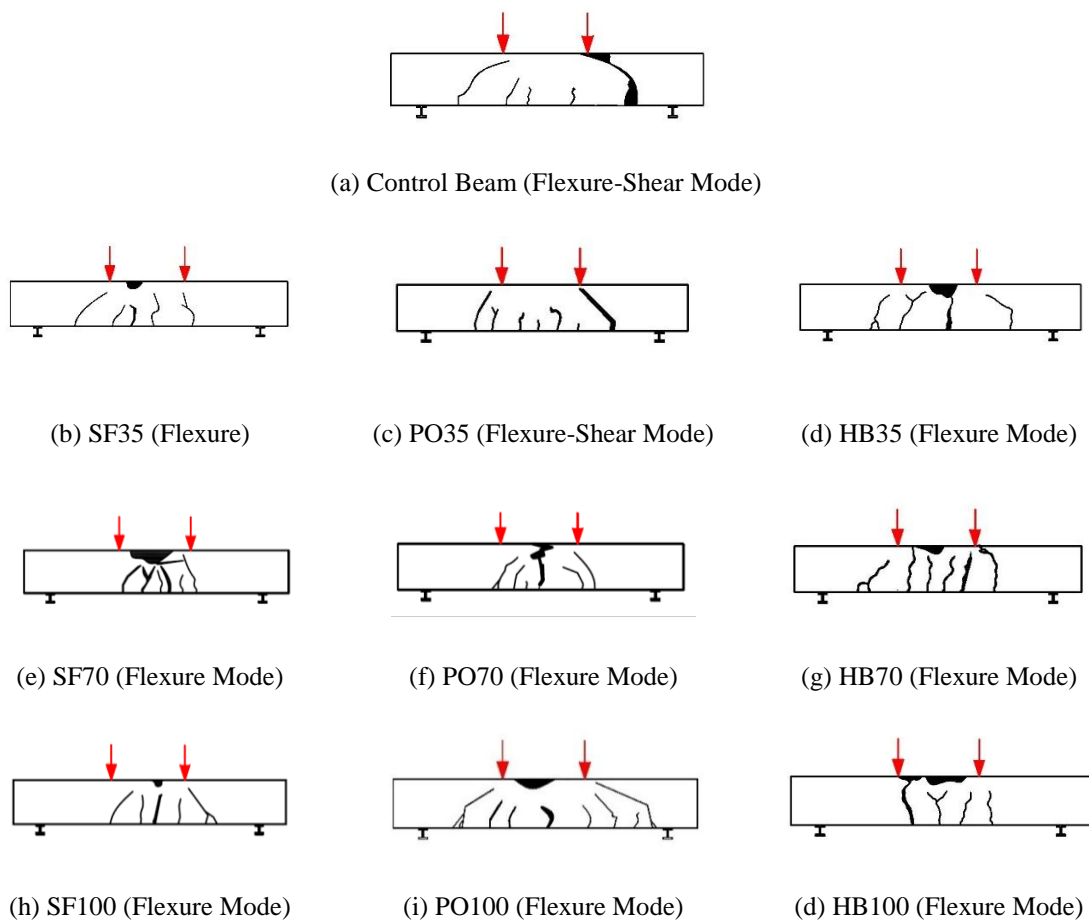


Figure 5.26: Failure modes of PSC beam with different fibers/dosages

In the case of 0.7% fiber dosage, the shear crack propagation in the PO70 specimen was arrested. PO70 failed in a dominant flexure failure similar to that of SF70 and HB70 specimens. With the increase in fiber dosage, significant crack branching and crack bridging in the fracture process zone was observed. At 1.0% fiber dosage, SF, PO, HB beams exhibited better ductility through fiber bridging action. HB100 failed in flexure at a displacement of 95mm, whereas the SF100 and PO100 did not fail even after reaching the actuator stroke capacity. Testing of both SF100 and PO100 was terminated at nearly 100 mm due to a limitation in the stroke capacity of the actuator. In summary, the presence of fibers enhanced the energy absorption and delayed propagation of cracks (fiber bridging action). Addition of fibers, in general, helped in improving the ductility through the formation of well-distributed cracks.

5.5.2. Comparison of load vs. strand strain variation

Strain gauges of 5mm gauge length were mounted on the strand at the mid-span of the prestressed concrete beam. During the pre-tensioning process, the strands were tensioned (4000 microns) within the elastic limit. Prestressing strands were cut after the concrete had attained sufficient strength (to resist the tensile stresses developed due to the eccentricity of the prestressing strand). The strain in the strands was continuously monitored, and losses in the strains were measured to be negligible. Figure 5.27 shows the strain variation in the prestressing strand during the testing. During the initial phase, i.e., before cracking, a major contributor to load resistance is the concrete in the cross-section. Thus, at initial loads before cracking, the strain variation in the strand (during testing) was negligible. However, once the load exceeds the cracking capacity of the specimen, the prestressing strand started contributing to load resistance. After cracking, the fiber reinforced specimen curves slightly shifted towards the load axis (Y-axis) due to the enhanced engagement of strand in resisting the loads. Due to

the higher cracking load in the HB specimen, the HB curves slightly shifted away from the SF and PO specimens. Strands are considered to yield at a strain of 10000 microns [33]. The complete load-strain behavior was not captured due to malfunctioning of the strain gauges after certain loading.

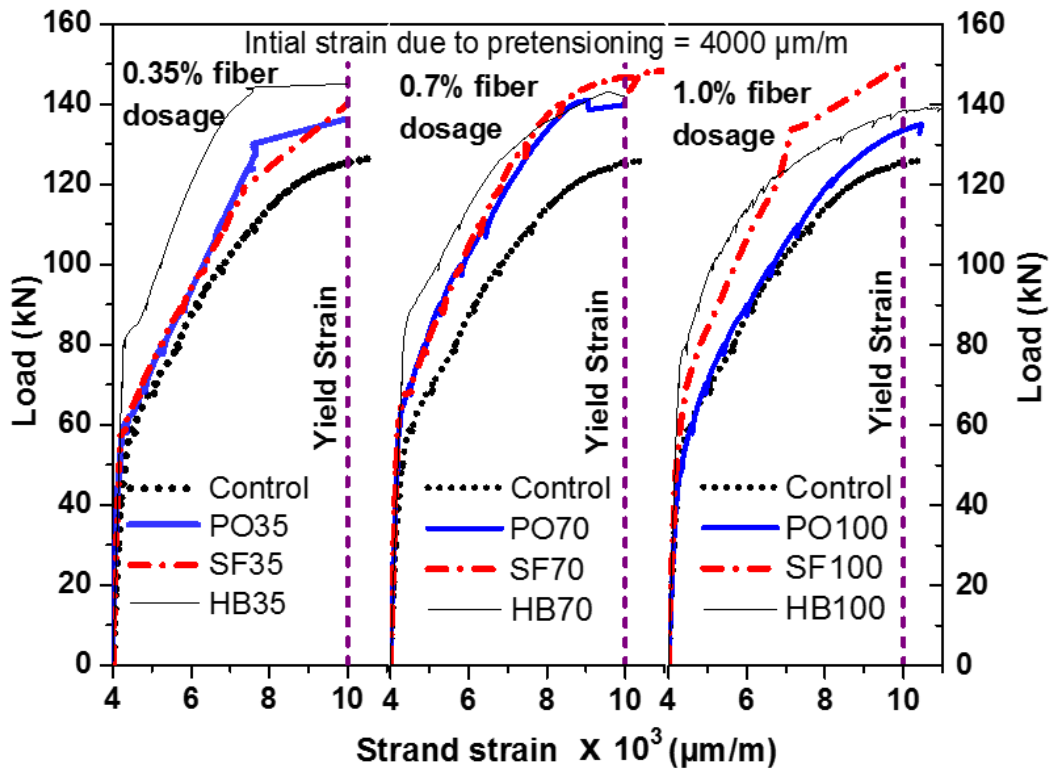


Figure 5.27: Load-strain (strand) behavior of PSC beams

5.5.3. Comparison of normalized strain energy absorption capacity

The flexural toughness/ductility of different fiber reinforced specimen is evaluated by energy absorbed by the specimen throughout the test. The energy absorption capacity of the specimen is calculated from the area under the load-deflection curve. Since the ultimate deflection values in the calculation of strain energy were different for each specimen, the strain energy values were normalized [34] for each specimen with their respective ultimate displacement values.

The normalized strain energy results are presented in Figure 5.28. The control specimen failed at lesser ultimate displacement with the flexure-shear mode which resulted in lesser energy absorption compared to the fiber-reinforced specimens. In the case of fiber-reinforced specimens, failure was delayed due to crack branching (multiple crack formation) and crack bridging effect provided by the fiber. Thus, they had higher energy absorption. At low fiber dosages, hybrid and steel fiber reinforced specimens had comparable normalized energy absorption capacity. At high fiber dosage of 1.0%, steel specimens had superior energy absorption compared to synthetic and hybrid fiber reinforced specimens.

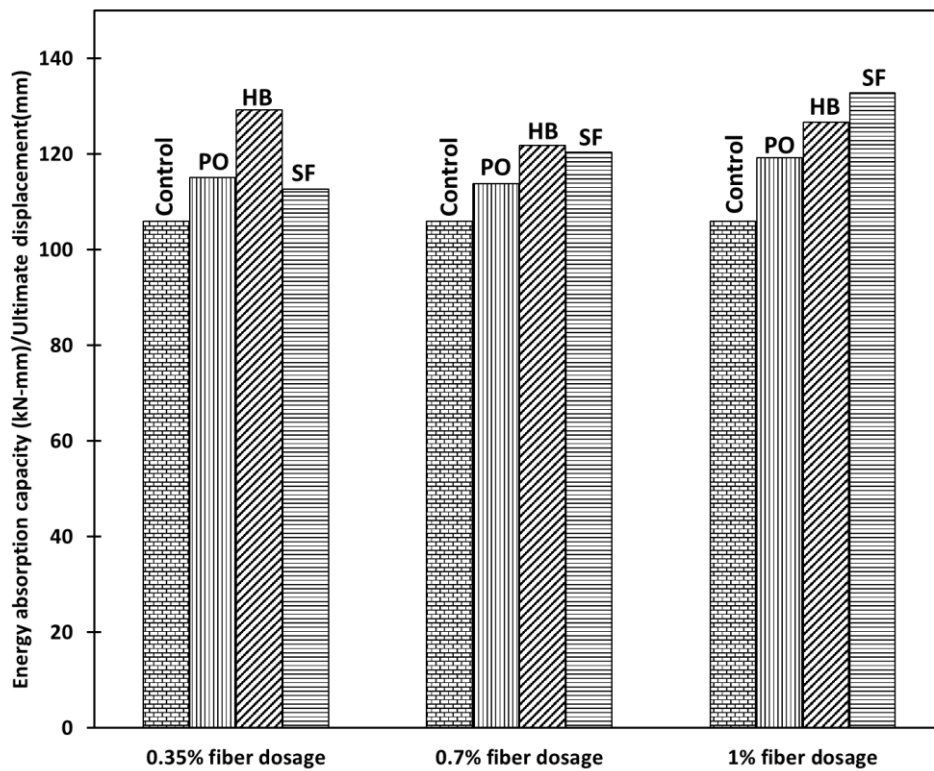


Figure 5.28: Normalized energy absorption capacity of the specimens

Chapter 6

Analytical Study

6.1. General

This chapter describes the capacity calculations of the fiber reinforced prestressed concrete beams of the current test program using RILEM recommendation. In the subsequent section, parameters affecting the cracking behavior such as crack width and crack spacing is also studied using RILEM TC-162-TDF [17], CEB-FIP modal code [35] and Moffat's crack spacing model [36].

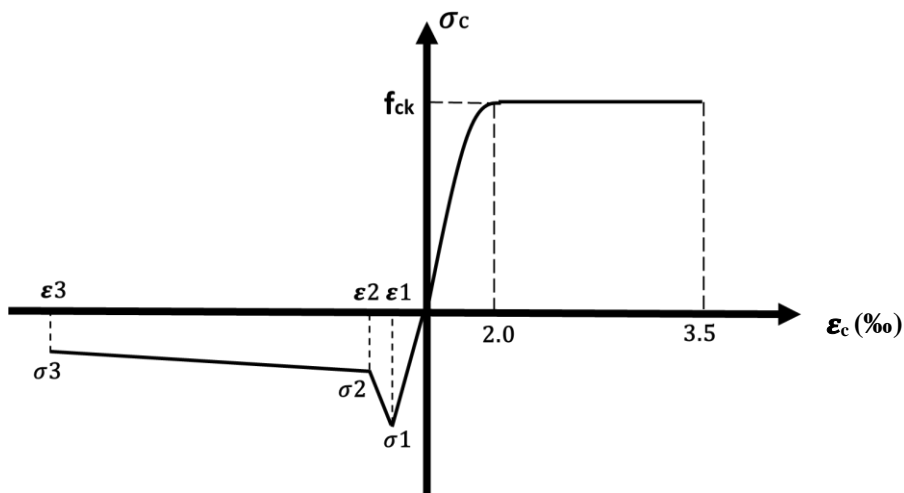
6.2. Capacity calculation using RILEM recommendations

Only limited models and recommendations are available for capacity calculations of synthetic and hybrid (SF+PO) fiber reinforced concrete specimens. In this study, RILEM recommendations, which were originally developed for steel fiber reinforced concrete are employed for strength calculations of synthetic, and hybrid fiber reinforced specimens. Additional information from compression and fractures tests were used in the calculations. The comparison of experimental and analytical capacities are presented in Table 6.1.

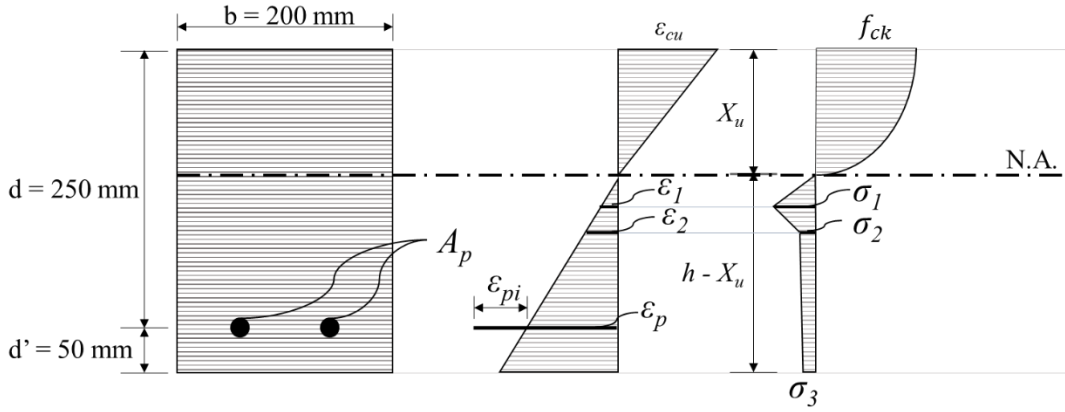
6.2.1. Flexural moment capacity

A MATLAB based nonlinear sectional analysis code based on a layer-by-layer approach was developed to estimate the ultimate moment of the section. For compression behavior of FRC, the RILEM recommendation [17] utilizes the design stress-strain curve, where the post-peak behavior was assumed plastic, and the before the peak is of parabolic in nature (Figure 6.1a).

The influence of fiber type on compression behavior was assumed to be negligible. As the fibers are assumed to contribute significantly in tension, their contribution to tensile resistance was included. The tensile stress-strain curve of fiber reinforced concrete under tension was included. The tensile stress-strain curve of fiber reinforced concrete under tension was obtained indirectly from fracture test results (Figure 5.1). The relation between residual strength values (fracture test) and the tensile stresses are presented in equation (6.1-6.3). For different dosage of fibers, the stress-strain relationship under tension was obtained by interpolating the results presented in Figure 5.1. In this approach of analysis, the cross section is discretized into a number of layers to obtain the uniform strain variation within each layer. Initially, the compressive top fiber strain is assumed, and the depth of the neutral axis is iterated to satisfy force equilibrium. The analytical estimates are compared with experimental ultimate moment capacity (Table 6.1).



a) Concrete stress-strain behavior under compression and tension



b) Layer by layer (fiber discretization) approach

Figure 6.1: Flexural capacity calculation

$$\sigma_1 = 0.7 f_{fctm,fl}(1.6 - d) \quad (6.1)$$

$$\sigma_2 = 0.45 f_{R,1} K_h \quad (6.2)$$

$$\sigma_3 = 0.37 f_{R,4} K_h \quad (6.3)$$

$$\varepsilon_1 = \sigma_1 / E_c \quad (6.4)$$

$$\varepsilon_2 = \varepsilon_1 + 0.1 \text{ ‰} \quad (6.5)$$

$$\varepsilon_3 = 25 \text{ ‰}$$

$$K_h = 1.0 - 0.6 \frac{h \text{ (cm)} - 12.5}{47.5} \quad [12.5 \text{ cm} \leq h \leq 60 \text{ cm}]$$

where

$f_{fctm,fl}$ = Mean flexural tensile strength in MPa

$f_{R,1}, f_{R,4}$ = are residual flexural strength of FRC at CMOD of 0.5mm and 3.5mm respectively

E_c = Modulus of elasticity of concrete

K_h = Size factor

h = overall depth (mm)

6.2.2. Shear capacity

RILEM recommendations are used to calculate the design shear capacity of the fiber reinforced prestressed concrete beams. Shear resistance is mainly due to three components (Figure 6.2) namely (i) shear resistance of the concrete member without shear reinforcement (V_{cd}) which includes resistance from uncracked concrete section (V_{cd1}), aggregate interlock (V_{cd2}) and dowel resistance (V_{cd3}), (ii) contribution of the steel/synthetic fibers (V_{fd}), and (iii) contribution of the shear reinforcement due to stirrups or inclined bars (V_{wd}). The shear strength of FRC is higher than that of the control specimen (without fibers). The shear strength increase is due to controlled crack propagation in the fracture process zone (FPZ) in fiber reinforced concrete. The crack bridging action improves the aggregate interlock as well, due to which shear capacity is enhanced in case of fiber reinforced concrete specimen. However, fibers failed to transfer stresses across the crack in traction free micro-crack zone. The following equations (6.6) to (6.16) are used in the calculations of shear capacity of prestressed fiber reinforced concrete beams. The calculated shear capacities are summarized and compared with experimental results in Table 6.1.

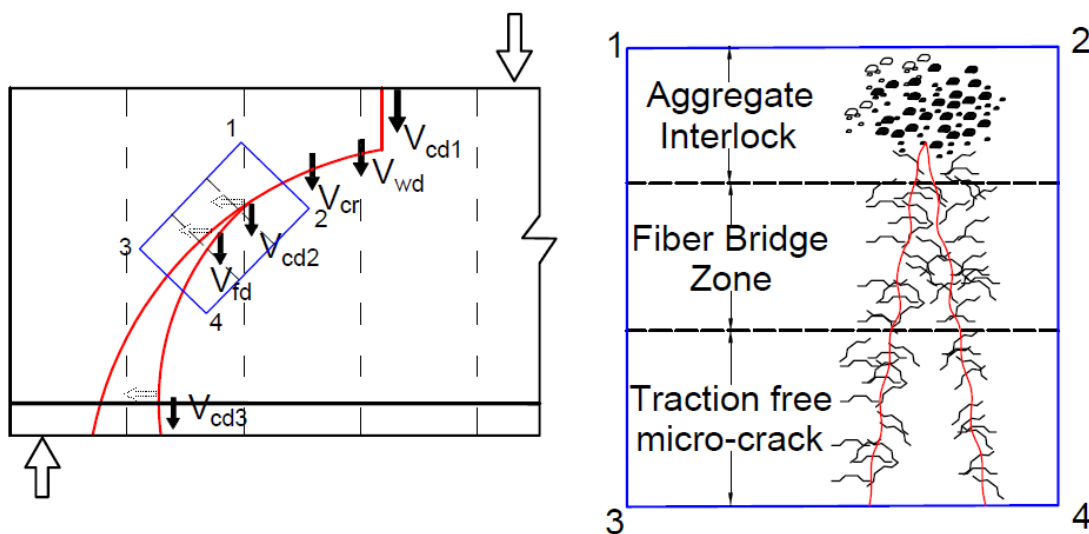


Figure 6.2: Shear resistance of FRC

$$V_{Rd3} = V_{cd} + V_{fd} + V_{wd} \quad (6.6)$$

$$V_{cd} = \left[0.12k(100\rho_l f_{ck})^{\frac{1}{3}} + 0.15\sigma_{cp} \right] b_w d \quad (N) \quad (6.7)$$

$$k = 1 + \sqrt{\frac{200}{d}} \quad (d \text{ in mm}) \quad \text{and} \quad k \leq 2 \quad (6.8)$$

$$\rho_l = \frac{A_s}{b_w d} \leq 2\% \quad (6.9)$$

$$\sigma_{cp} = \frac{N_{sd}}{A_c} \quad (6.10)$$

$$V_{fd} = k_f k_1 \tau_{fd} b_w d \quad (N) \quad (6.11)$$

$$k_f = 1 + n \left(\frac{h_f}{b_w} \right) \left(\frac{h_f}{d} \right) \quad \text{and} \quad k_f \leq 1.5 \quad (6.12)$$

$$n = \frac{b_f - b_w}{h_f} \quad \text{where} \quad n \leq 3 \quad \text{and} \quad n \leq \frac{3b_w}{h_f} \quad (6.13)$$

$$k_1 = \frac{1600 - d}{1000} \quad (d \text{ in mm}) \quad \text{and} \quad k_1 \geq 1 \quad (6.14)$$

$$\tau_{fd} = 0.12 f_{Rk,4} \quad (6.15)$$

$$V_{wd} = \frac{A_{sw}}{s} 0.9 d f_{ywd} (1 + \cot \alpha) \sin \alpha \quad (N) \quad (6.16)$$

where

f_{ck} = Characteristic compressive strength of cylinders in MPa

E_c = Modulus of elasticity of concrete

A_c = cross section of concrete (mm²)

A_s = Area of tension reinforcement extending not less than “d + anchorage length” beyond the section considered (mm²).

A_{sw} = Area of shear reinforcement (mm²).

- b_f = The width of the flanges (mm)
- b_w = Minimum width of the section over the effective depth d (mm).
- d = effective depth (mm)
- $f_{rk,4}$ = The residual flexural tensile strengths at $CMOD = 3.5mm$
- f_{ywd} = Design yield strength of the shear reinforcement (N/mm^2).
- h = overall depth (mm)
- h_f = height of the flanges (mm)
- k_f = factor for taking into account the contribution of the flanges in a T-section
- N_{sd} = longitudinal force in section due to loading or prestressing
- s = spacing between the shear reinforcement measured along the longitudinal axis (mm)
- V_{cd} = the shear resistance of the member without shear reinforcement
- V_{fd} = Shear contribution of the steel/synthetic fiber shear reinforcement
- V_{Rd3} = the design shear resistance of a section of a beam
- V_{wd} = Shear contribution of the shear reinforcement due to stirrups and/or inclined bars
- α = angle of the shear reinforcement with the longitudinal axis
- τ_{fd} = design value of the increase in shear strength due to steel/synthetic fibers

6.2.3. Capacity comparison

The experimentally observed capacity of fiber reinforced prestressed concrete beams are compared with the analytical capacity obtained from the RILEM recommendation [17] and are presented in Table 6.1. It can be observed that shear capacity calculated from RILEM recommendation is higher than that of flexural capacity. The use of RILEM recommendations, in general, resulted in a conservative estimate of the flexural capacity of hybrid fiber reinforced prestressed concrete beams.

Table 6.1: Capacity comparison

| | Control | SF35 | PO35 | HB35 | SF70 | PO70 | HB70 | SF100 | PO100 | HB100 |
|-----------------------------------------------------|---------|--------|--------|--------|--------|--------|--------|--------|--------|--------|
| | 0.00% | 0.35% | | | 0.70% | | | 1.00% | | |
| Ultimate load, P_{ul} (kN) | 130.00 | 143.00 | 136.80 | 145.20 | 146.00 | 139.70 | 140.60 | 159.00 | 135.10 | 141.70 |
| Load corresponding to flexural capacity(kN) (RILEM) | 111.63 | 117.04 | 113.36 | 114.32 | 122.53 | 115.55 | 115.01 | 126.40 | 117.90 | 116.88 |
| Load corresponding to shear capacity(kN) (RILEM) | 140.88 | 166.76 | 146.94 | 155.58 | 186.52 | 151.86 | 159.98 | 203.06 | 164.26 | 171.84 |

6.3. Analysis of crack width and crack spacing in fiber reinforced concrete beams

6.3.1. Introduction

Cracking of concrete is inevitable in concrete structures. However, this aspect is considered only to quantify durability, serviceability of reinforced concrete structures. Moreover, serviceability limit state design methods suggest having some well-distributed cracks rather than very few wider cracks in a structure. Furthermore, in the case of fiber reinforced concrete, the crack width and cracked spacing are the input parameters [37] to predict the mechanical behavior of the members using models such as modified compression field theory (MCFT) and distributed stress field model (DSFM). There are several methods available in different codes to calculate the crack width and crack spacing. These two parameters (crack width and crack spacing) are subjected to scatter wide. Hence, all the available methods formulations are an attempt to predict the probable maximum crack width and spacing.

The main causes of cracking can be listed as a) bending, direct tension causes the flexural cracking b) shear or torsion causes the diagonal tension cracks, c) creep and shrinkage of concrete. Parameters affecting crack width are i) tensile stress in rebar ii) concrete cover, iii) rebar spacing in concrete, iv) member depth and location of neutral axis v) tensile strength of concrete, vi) bond strength between rebar and concrete. For the current case of fiber reinforced prestressed concrete beam (Figure 6.3), crack widths are calculated in the post-cracking range at the serviceability regime. The results from the sectional analysis using RILEM recommendations [17] are presented in Figure 6.4. In this case, crack widths are calculated in the range between 40 kN-m and 65 kN-m.

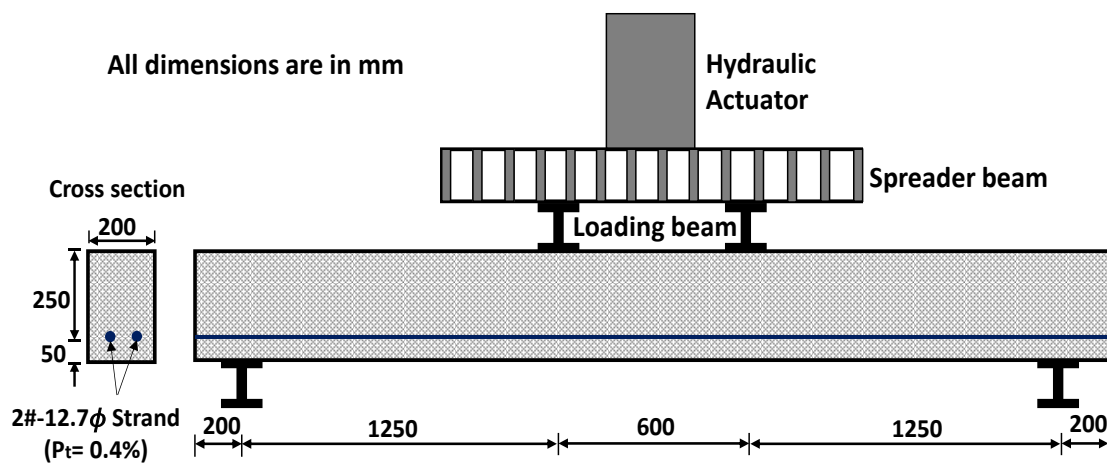


Figure 6.3: Fiber reinforced prestressed concrete beam details

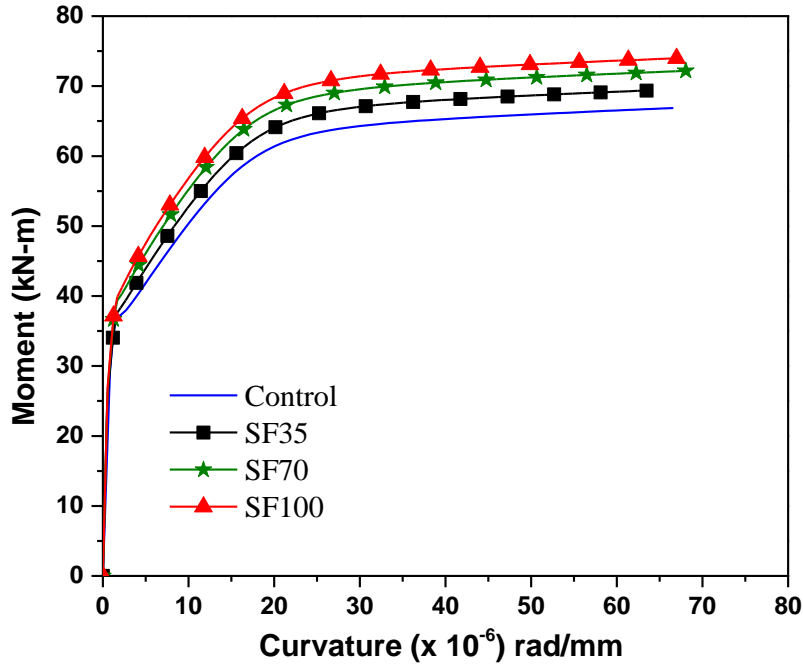


Figure 6.4: Result from sectional analysis using RILEM recommendations

6.3.2. Crack spacing model based on RILEM TC162-TDF

In this model, the crack width calculations are similar to that of reinforced concrete without fibers. Just after the cracking, the tensile stress in fiber reinforced concrete (FRC) is given by $0.45 f_{Rm,1}$ ($f_{Rm,1}$ - the residual tensile strength of FRC at 0.5mm CMOD value) and this value is assumed to be constant over the cracked part of the section. The crack width is directly proportional to crack spacing and mean stress in steel rebar, and is given by

$$w_k = \beta s_{rm} \varepsilon_{sm} \quad (6.17)$$

w_k = the design crack width (mm)

s_{rm} = average final crack spacing (mm)

$\beta = 1.3$ for restrained cracking in sections with a minimum depth, breadth or thickness of 300 mm or below

$$\varepsilon_{sm} = \frac{\sigma_s}{E_s} \left[1 - \beta_1 \beta_2 \left(\frac{\sigma_{sr}}{\sigma_s} \right)^2 \right] \quad (6.18)$$

σ_s = the stress in the tensile reinforcement calculated based on cracked section (N/mm²)

σ_{sr} = stress in tensile reinforcement calculated based on a cracked section under the loading condition causing first cracking (N/mm²)

β_1 = coefficient for bond properties of bars = 1.0 for high bond bars

β_2 = a coefficient which takes into account of the duration of loading = 1.0 for short term loading

Average crack spacing is given by

$$s_{rm} = \left(50 + 0.25k_1k_2 \frac{\phi_b}{\rho_r} \right) \cdot \left(\frac{50}{L} \right) \quad (\text{mm}) \quad \left(\frac{50}{L} \right) \leq 1 \quad (6.19)$$

ϕ_b = bar size in mm

k_1 = coefficient which takes account of bond properties (0.8 for high bond bars, 1.6 for plain bars)

k_2 = a coefficient which takes into the account of the form of strain distribution (0.5 for bending, 1.0 for pure tension)

ρ_r = effective reinforcement ratio, $A_s/A_{c,eff}$ where A_s is the area of reinforcement contained within the effective tension area $A_{c,eff}$

L = length of steel fiber

ϕ = Diameter of steel fiber (mm)

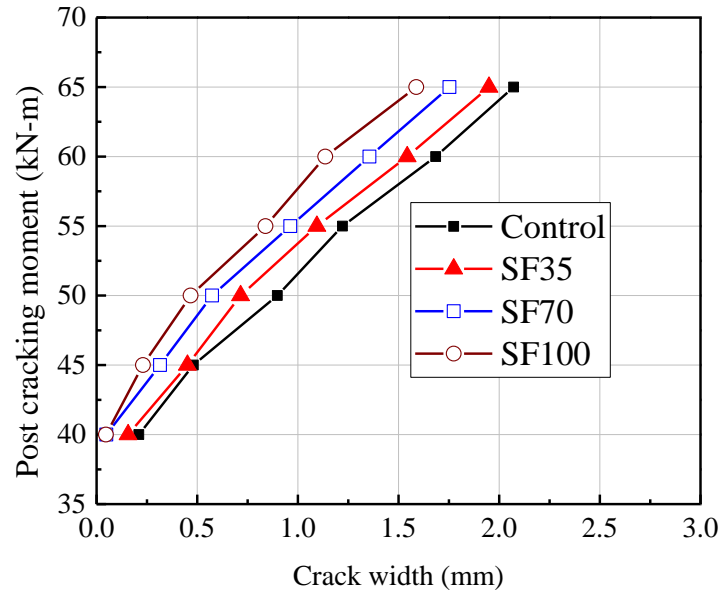


Figure 6.5: Crack width calculation using RILEM(Euro code) recommendation

From Figure 6.5 it can be observed that the crack width of steel fiber reinforced specimens lies in the range between 0 to 2mm. At some load level, it can be observed that the crack width reduces with the increase in fiber dosage.

6.3.3. Crack spacing model based on CEB-FIP modal code

CEB-FIP modal code [35] consists of two crack spacing formulations, i) initial unstable cracking phase ii) stabilized cracking phase. At the serviceability stage, the stabilized cracking phase exists. Hence, the formulations related to the stabilized cracking phase is used for the current study. Crack spacing is given by

$$S_m = \frac{2}{3} \cdot \frac{\phi_b}{3.6\rho_r} \quad (6.20)$$

Where

ϕ_b = bar size in mm

ρ_r = effective reinforcement ratio, $A_s/A_{c,eff}$ where A_s is the area of reinforcement contained within the effective tension area $A_{c,eff}$

From Figure 6.6, it can be observed that in the serviceability region the crack width varies in the range of 0-3mm for all fiber reinforced specimen. As the fiber dosage is increased, the corresponding crack width reduced significantly.

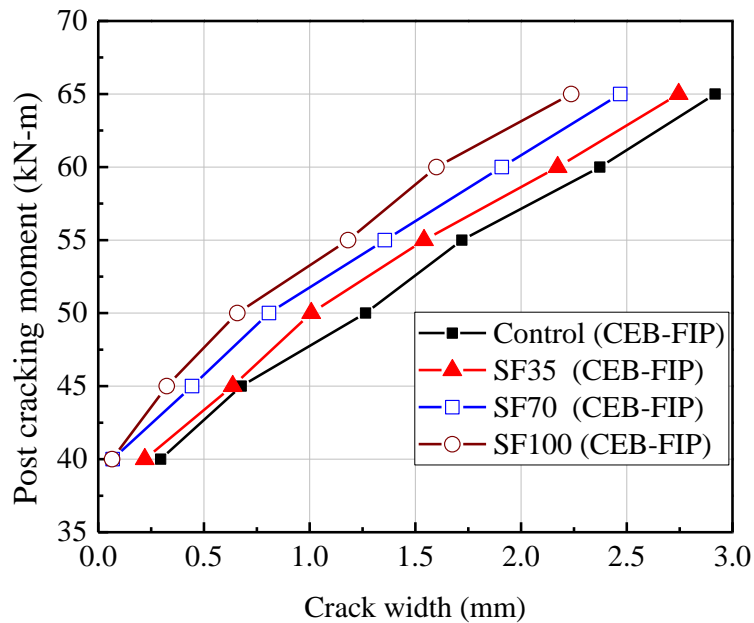


Figure 6.6: Crack width calculation using CEB-FIP (1993)

6.3.4. Modified equations based on Moffatt's crack spacing model

The drawback of the previously presented model (Euro code and CEB-FIP code (1993)) is that fiber properties such as aspect ratio, fiber dosage are not explicitly included in the formulations. Hence the Moffat [36] proposed modification factor (equation 6.21 and 6.22) regarding residual flexural tensile strength (defined as the ratio of post cracking residual flexural strength of FRC to the cracking strength). The variation of crack width in the post-cracking phase as per the Moffat's model is presented in Figure 6.7.

Modified Euro code

$$s_{rm} = \left(50 + 0.25k_1k_2 \frac{\phi_b}{\rho_r} \right) \cdot \left(1 - \frac{f_{res}}{f_{cr}} \right) \quad (6.21)$$

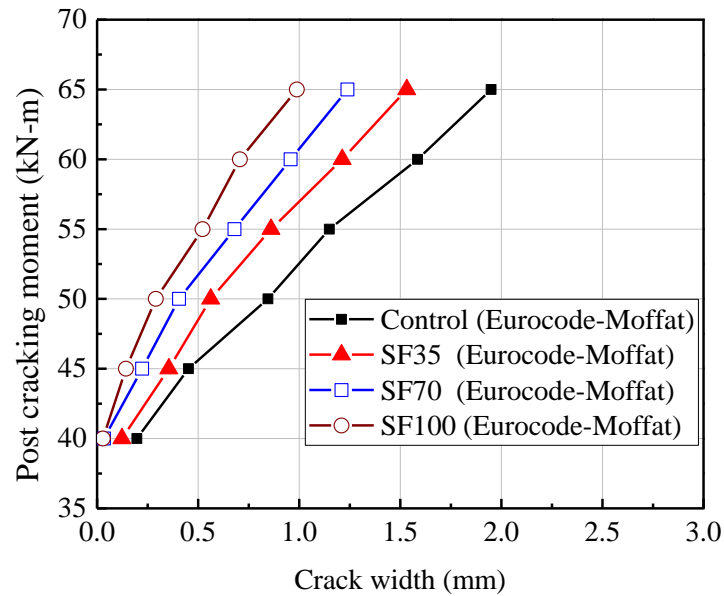
Modified CEB-FIP (1993) is as follows (stabilized cracking phase)

$$S_m = \frac{2}{3} \cdot \frac{\phi_b}{3.6\rho_r} \cdot \left(1 - \frac{f_{res}}{f_{cr}} \right) \quad (6.22)$$

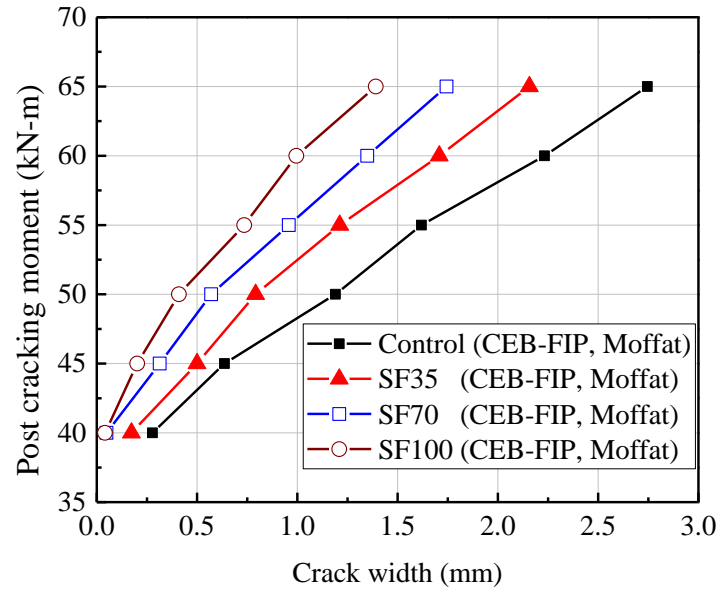
where

f_{res} = post cracking tensile strength of concrete (MPa)

f_{cr} = cracking stress of the concrete (MPa)



a) Crack width based on the modified Euro code (Moffatt's factor)

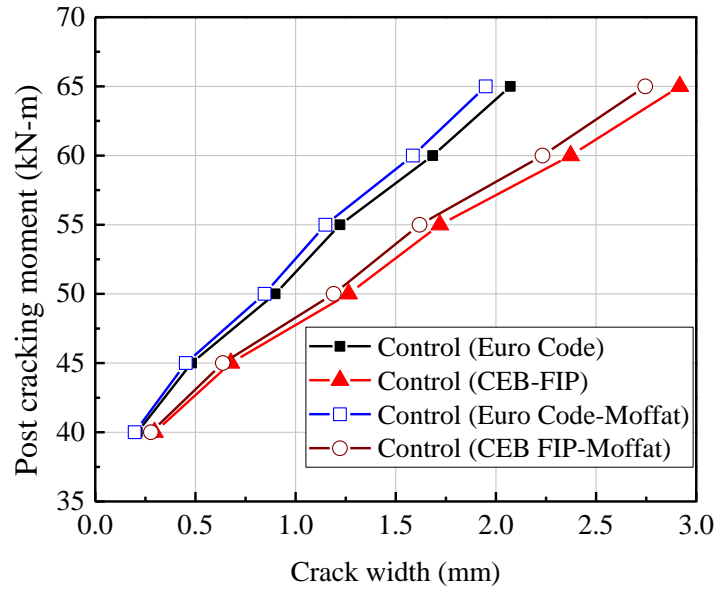


b) Crack width based on modified CEB-FIP modal code (Moffatt's factor)

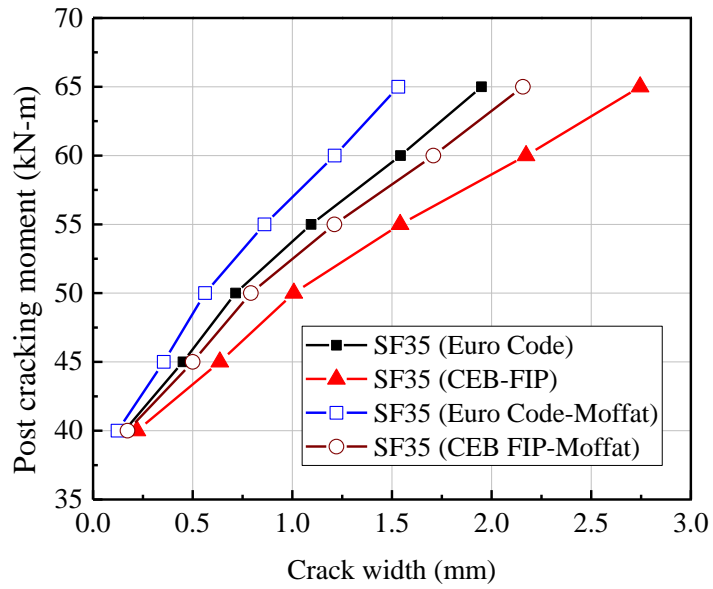
Figure 6.7: Moffatt's model

6.3.5. Effect of modification factor in the formulae of RILEM and CEB-FIP code

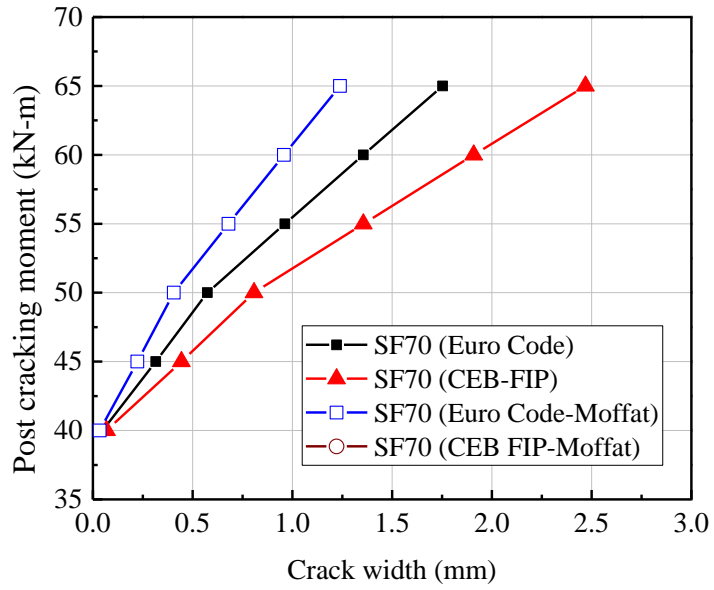
In this section previously presented results, with and without modification factor are compared at the same fiber dosage to evaluate the effect of Moffatt's modification factor in the formulations. At the same fiber dosage, all the results of RILEM and CEB-FIP modal code are plotted as shown in Figure 6.8. In the case of control specimen, residual strength influence is very minimum, hence in Figure 6.8a both the curves (with and without Moffatt's factor) follow a similar path. Whereas in the case of fiber reinforced specimen the difference between the curves is significant (Figure 6.8).



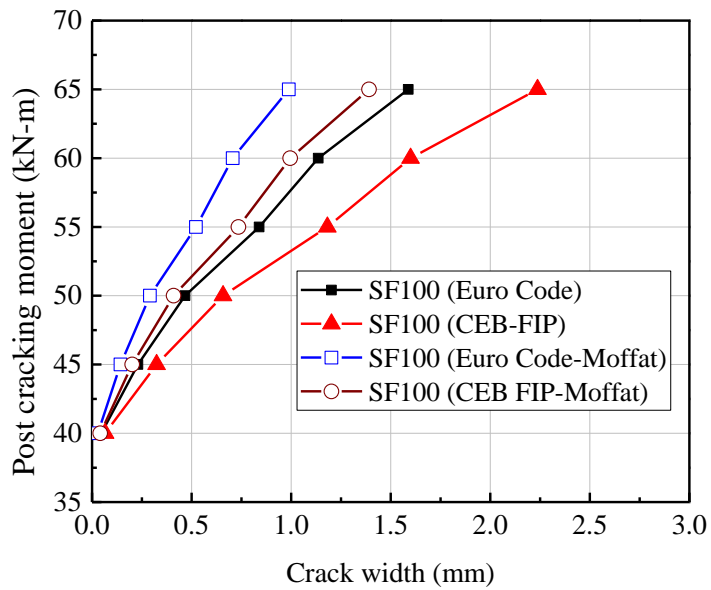
a) Effect of Moffat's factor in the control specimens



b) Effect of Moffat's factor in SF35 specimens



c) Effect of Moffat's factor in SF70 specimens



d) Effect of Moffat's factor in SF100 specimens

Figure 6.8: Influence of Moffat's modification factor

Chapter 7

Summary and Conclusions

Pre-tensioned prestressed concrete beams with and without steel and synthetic fibers were cast and tested at four-point bending configuration to evaluate the role of different fibers on flexure-shear behavior, crack bridging effect and serviceability performance. The main motivation behind the use of hybrid fiber reinforced concrete is to attain maximum post-cracking resistance at minimum fiber dosage without compromising the workability in the fresh state. Only limited fiber dosages and their combinations have been considered in this study. The hybrid effect between the fibers (steel, synthetic fibers), volume fraction and aspect ratio of fibers can be significant on the constitutive behavior under both tension and compression. Also, the effect of concrete strength, prestressing levels, shear span to depth ratio and shear reinforcement ratio would also influence the effect of hybrid FRC on the flexure-shear behavior of prestressed concrete beams. Understanding these aspects is the scope for further work. The following conclusions can be made from the results presented in this work:

- Though the addition of steel, synthetic and hybrid fibers showed marginal improvement in the peak strength, it resulted in very good improvement in strain energy-based ductility of the prestressed concrete beams. The major contribution of fibers was in bridging the cracked surfaces which resulted in improved post-cracking stiffness and higher ultimate deflection. The strain in the strand reduced due to the addition of steel fibers in the post-cracking regime.
- Fiber inclusion to concrete significantly influenced the failure mode of the prestressed concrete beams. At 0.35% fiber dosage, the failure mode changed from flexure-shear

to ductile flexure mode in the case of steel and hybrid fiber reinforced beams. This change in failure mode occurred at 0.7% fiber dosage in synthetic fiber reinforced beams due to the lower elastic modulus of the synthetic fibers.

- Distribution of cracks increased with an increase in the addition of steel fibers. The post-cracking behavior of hybrid fiber reinforced specimens lies in between steel and synthetic fiber reinforced specimens.
- Presence of the synthetic fiber alone did not influence the cracking capacity of the specimen. However, steel (SF) and hybrid fibers (SF+PO) restricted the crack initiation, thereby marginally improved the cracking strength of the PSC beams.
- The flexural toughness of the prestressed concrete beams was improved due to the fiber addition. The normalized strain energy clearly shows that hybrid fibers performed comparably to that of steel fibers at low dosage. At a higher dosage of 1.0%, steel fiber reinforced beams had higher toughness when compared to synthetic and hybrid fiber reinforced ones.
- DIC measurements correlated well with conventional measurements of displacement sensors. The reduction in peak strain in tensile fibers was up to 50% due to the crack bridging mechanism of steel fibers.
- The capacity of the prestressed concrete beams with different fibers was calculated using RILEM recommendations, which resulted in a conservative estimate of the test specimen.
- The crack widths calculated employing the recommendations of Euro code and CEB-FIP (1993) code for steel fiber reinforced prestressed concrete specimens reduced with the increase in fiber dosage.

- Euro code and CEB-FIP (1993) code formulations explicitly do not consider the fiber properties (length and aspect ratio of fiber) and volume fraction. Hence Moffat modification factor, which indirectly considers the volume fraction and aspect ratio is also used to compute the crack width.

References

- [1] ACI Committee 318, *Building Code Requirements for Structural Concrete (ACI 318-08)*, vol. 2007. 2008.
- [2] M. A. Rasheed and S. S. Prakash, “Mechanical behavior of sustainable hybrid-synthetic fiber reinforced cellular light weight concrete for structural applications of masonry,” *Constr. Build. Mater.*, vol. 98, pp. 631–640, 2015.
- [3] A. B. Bhosale, M. A. Rasheed, S. S. Prakash, and G. Raju, “A study on the efficiency of steel vs. synthetic vs. hybrid fibers on fracture behavior of concrete in flexure using acoustic emission,” *Constr. Build. Mater.*, vol. 199, pp. 256–268, 2019.
- [4] S. Jain, S. S. Prakash, and K. V. L. Subramaniam, “Monitoring of Concrete Cylinders With and Without Steel Fibers Under Compression Using Piezo-Ceramic Smart Aggregates,” *J. Nondestruct. Eval.*, vol. 35, no. 4, pp. 1–7, 2016.
- [5] G. Srikar, G. Anand, and S. Suriya Prakash, “A Study on Residual Compression Behavior of Structural Fiber Reinforced Concrete Exposed to Moderate Temperature Using Digital Image Correlation,” *Int. J. Concr. Struct. Mater.*, vol. 10, no. 1, pp. 75–85, 2016.
- [6] A. Bentur, “Cementitious composites,” *Composites*, vol. 10, no. 1, p. 53, 1979.
- [7] T. No, “How Safe are Our Large Reinforced Concrete Beams?,” *ACI J. Proc.*, vol. 64, no. 3, 1967.
- [8] Y. Ding, Z. You, and S. Jalali, “The composite effect of steel fibres and stirrups on the shear behaviour of beams using self-consolidating concrete,” *Eng. Struct.*, vol. 33, no. 1, pp. 107–117, 2011.
- [9] D. Y. Yoo, Y. S. Yoon, and N. Banthia, “Flexural response of steel-fiber-reinforced concrete beams: Effects of strength, fiber content, and strain-rate,” *Cem. Concr. Compos.*, vol. 64, pp. 84–92, 2015.
- [10] H. Singh, “Flexural Modeling of Steel Fiber-Reinforced Concrete Members: Analytical Investigations,” *Pract. Period. Struct. Des. Constr.*, vol. 20, no. 4, p. 04014046, 2015.
- [11] D. R. Sahoo and A. Sharma, “Effect of steel fiber content on behavior of concrete beams with and without stirrups,” *ACI Struct. J.*, vol. 111, no. 5, pp. 1157–1166, 2014.

- [12] A. P. Fantilli, H. Mihashi, and P. Vallini, "Post-peak behavior of cement-based materials in compression," *ACI Mater. J.*, vol. 104, no. 5, pp. 501–510, 2007.
- [13] M. H. Harajli, "Bond Behavior in Steel Fiber-Reinforced Concrete Zones under Static and Cyclic Loading: Experimental Evaluations and Analytical Modeling," *J. Mater. Civ. Eng.*, vol. 22, no. 7, pp. 674–686, 2010.
- [14] M. Y. Abbas and M. I. Khan, "Fiber-Matrix Interfacial Behavior of Hooked-End Steel Fiber-Reinforced Concrete," *J. Mater. Civ. Eng.*, vol. 28, no. 11, p. 04016115, 2016.
- [15] A. M. Alhozaimy, P. Soroushian, and F. Mirza, "Mechanical properties of polypropylene fiber reinforced concrete and the effects of pozzolanic materials," *Cem. Concr. Compos.*, vol. 18, no. 2, pp. 85–92, 1996.
- [16] A. Yazdanbakhsh, S. Altoubat, and K. A. Rieder, "Analytical study on shear strength of macro synthetic fiber reinforced concrete beams," *Eng. Struct.*, vol. 100, pp. 622–632, 2015.
- [17] RILEM TC 162-TDF, " σ - ϵ - design method - Final Recommendation," *Mater. Struct.*, vol. 36, no. October, pp. 560–567, 2003.
- [18] FIB-Fédération Internationale du Béton. Model Code 2010 (first complete draft), bulletin 55, vol. 1(5) "Materials." Lausanne 2010.
- [19] A. Amin, S. J. Foster, R. I. Gilbert, and W. Kaufmann, "Material characterisation of macro synthetic fibre reinforced concrete," *Cem. Concr. Compos.*, vol. 84, pp. 124–133, 2017.
- [20] W. Yao, J. Li, and K. Wu, "Mechanical properties of hybrid fiber-reinforced concrete at low fiber volume fraction," *Cem. Concr. Res.*, vol. 33, no. 1, pp. 27–30, 2003.
- [21] S. J. Lee and J. P. Won, "Flexural behavior of precast reinforced concrete composite members reinforced with structural nano-synthetic and steel fibers," *Compos. Struct.*, vol. 118, no. 1, pp. 571–579, 2014.
- [22] D. R. Sahoo, A. Solanki, and A. Kumar, "Influence of Steel and Polypropylene Fibers on Flexural Behavior of RC Beams," *ASCE J. Mater. Civ. Eng.*, vol. 08, no. Aci 2008, pp. 1–9, 2014.
- [23] G. Tiberti, F. Minelli, G. A. Plizzari, and F. J. Vecchio, "Influence of concrete strength

- on crack development in SFRC members,” *Cem. Concr. Compos.*, vol. 45, pp. 176–185, 2014.
- [24] E. Cuenca and P. Serna, “Shear behavior of prestressed precast beams made of self-compacting fiber reinforced concrete,” *Constr. Build. Mater.*, vol. 45, pp. 145–156, 2013.
- [25] E. Cuenca and P. Serna, “Failure modes and shear design of prestressed hollow core slabs made of fiber-reinforced concrete,” *Compos. Part B Eng.*, vol. 45, no. 1, pp. 952–964, 2013.
- [26] S. K. Padmarajaiah and A. Ramaswamy, “Flexural strength predictions of steel fiber reinforced high-strength concrete in fully/partially prestressed beam specimens,” *Cem. Concr. Compos.*, vol. 26, no. 4, pp. 275–290, 2004.
- [27] S. K. Padmarajaiah and A. Ramaswamy, “Crack-width prediction for high-strength concrete fully and partially prestressed beam specimens containing steel fibers,” *ACI Struct. J.*, vol. 98, no. 6, pp. 852–861, 2001.
- [28] A. Conforti, F. Minelli, and G. A. Plizzari, “Shear behaviour of prestressed double tees in self-compacting polypropylene fibre reinforced concrete,” *Eng. Struct.*, vol. 146, pp. 93–104, 2017.
- [29] IS 1343, Code of Practices for Prestressed Concrete, Bureau of Indian Standards, New Delhi, India, 1980.
- [30] IS 10262, Proportioning-Guideline, Indian Standard Concrete Mix, Bureau of Indian Standards, New Delhi, India, 2009.
- [31] BS EN 14651, “Test method for metallic fibred concrete — Measuring the flexural tensile strength (limit of proportionality (LOP), residual),” *Br. Stand. Inst.*, vol. 3, pp. 1–17, 2005.
- [32] Schreier, Hubert, Jean-José Orteu, and Michael A. Sutton. Image correlation for shape, motion and deformation measurements. Springer US, 2009.
- [33] R. K. Devalapura, “Stress-Strain Modeling of Prestressing Strands,” vol. 9, no. 270, pp. 100–106.
- [34] H. C. Mertol, E. Baran, and H. J. Bello, “Flexural behavior of lightly and heavily

- reinforced steel fiber concrete beams,” *Constr. Build. Mater.*, vol. 98, pp. 185–193, 2015.
- [35] CEB-FIP, “Model Code 1990 (Design Code),” Comité Euro-International du Béton, Lausanne, 1993.
- [36] K. Moffatt, “Analyse de Dalles de Pont avec Armature Réduite et Béton de Fibres Métalliques,” M.Sc.A Thesis, École Polytechnique de Montréal, 2001.
- [37] J. R. Deluce, “Cracking Behaviour of Steel Fibre Reinforced Concrete Containing Conventional Steel Reinforcement,” p. 506, 2011.

List of Publications

1. **Joshi, S.S.**, Thammishetti, N., Prakash, S.S. and Jain, S., “Cracking and Ductility Analysis of Steel Fiber-Reinforced Prestressed Concrete Beams in Flexure.” ACI Structural Journal, 115(6), 2018.
2. **Joshi, S.S.**, Thammishetti, N., and Prakash, S.S., “Efficiency of steel and macro-synthetic structural fibers on the flexure-shear behaviour of prestressed concrete beams.” Engineering Structures, 171, pp.47-55,2018.
3. **Joshi, S.S.**, Thammishetti, N., and Prakash, S.S., “Effect of Hybridization on the Flexure-Shear Behavior of Steel and Synthetic Fiber Reinforced Prestressed Concrete Beams.” ACI Structural Journal (Under review),2019.

Other contributions: Not included in thesis

1. Lakavath, C., Pidapa, V., **Joshi, SS.**, Prakash, SS., Kondraivendhan, B., “Shear behavior steel fiber reinforced precast prestressed concrete beams” Proceedings of ICCMS, Hyderabad, India,2018.
2. Lakavath, C., **Joshi, SS.**, Prakash, SS., “Effect of Steel Fibers on the Shear Crack-Width and Crack-Slip Behaviour of Prestressed Concrete Beams using Digital Image Correlation”, Engineering structures(Under review),2018.